

Flexible scheme for the implementation of nonadiabatic geometric quantum computationYi-Hao Kang^{1,2}, Zhi-Cheng Shi,^{1,2} Bi-Hua Huang,^{1,2} Jie Song,³ and Yan Xia^{1,2,*}¹*Department of Physics, Fuzhou University, Fuzhou 350116, China*²*Fujian Key Laboratory of Quantum Information and Quantum Optics (Fuzhou University), Fuzhou 350116, China*³*Department of Physics, Harbin Institute of Technology, Harbin 150001, China*

(Received 20 October 2019; accepted 21 February 2020; published 16 March 2020)

In this paper, a flexible and effective scheme is proposed to realize nonadiabatic geometric quantum gates with the invariant based reverse engineering and the nonadiabatic holonomic quantum computation (NHQC+) presented in recent work [B.-J. Liu *et al.*, *Phys. Rev. Lett.* **123**, 100501 (2019)] for extensible geometric quantum computation. The scheme provides variabilities for most of control parameters, and can build up multiple evolution paths with different geometric phases acquired in a cycling evolution. As the computational basis can be covered by the evolution paths, the realization of the nonadiabatic geometric quantum computation is possible without auxiliary levels. Moreover, multiple types of nonadiabatic geometric quantum gates can also be easily constructed by only adjusting boundary conditions of control parameters with the method. To show the applications of the scheme, we discuss the implementations of nonadiabatic geometric quantum gates of spin qubits in a double-quantum-dot system with numerical simulations. The results indicate that the scheme possesses robustness against the errors and noise. Therefore, the scheme may offer some interesting perspectives for the realization of the nonadiabatic geometric quantum computation.

DOI: [10.1103/PhysRevA.101.032322](https://doi.org/10.1103/PhysRevA.101.032322)**I. INTRODUCTION**

Quantum computation is one of the most important parts in the field of quantum information science, which has been shown as a promising candidate in solving many practical problems [1–5]. Since the implementations of the quantum gates are indispensable to the realization of the quantum computation, how to implement quantum gates with high accuracy and fast speed is a very hot topic in the past decades [6–10], and many interesting researches [11–17] based on different viewpoints have been put forward. The geometric quantum computation [18–25] is a very interesting concept that has arisen in the previous researches, which makes the use of the Abelian or non-Abelian geometric phases [26–29] of quantum states acquired in a cyclic evolution. Since the geometric phase is mainly depended on the global properties of the evolution paths, the geometric quantum gates are resistant to the influence of the local fluctuations [30–35]. This feature makes the geometric quantum computation receive increasing attention.

In the early implementations of geometric quantum gates, the geometric phases usually obtained in an adiabatic cycling evolution [18,21], where the variations of parameters should be slow enough to make sure the eigenvectors parallel evolve. The adiabatic evolution limits the speed of the gate implementations and causes continuous exposure of the system to the decoherence. Afterward, to accelerate the geometric quantum computation, the concept of the nonadiabatic geometric quantum computation been developed, and has subsequently been applied in the realization of different kinds of quantum

gates in many physical systems [36–47]. Because the nonadiabatic geometric quantum computation removes the limit of speed required by the adiabatic evolution, the gate implementations have shown the robustness against both noise and decoherence.

As a typical way to implement nonadiabatic geometric quantum gates, one can select a set of solutions of the Schrödinger equation and form a subspace. If the selected solutions satisfy both the cyclic evolution and the parallel transport conditions, then one can acquire a non-Abelian geometric phase [36,37] in the considered subspace. This approach is known as the nonadiabatic holonomic quantum computation (NHQC), which has been demonstrated to share all the holonomic nature of its adiabatic counterpart while being free of the long run-time requirement [48–50]. The merits of the NHQC can help to produce high-fidelity quantum gates. However, the parallel transport conditions may constrain the selections of control parameters in the Hamiltonian in some cases, which make NHQC sometimes relatively complex to combining with some quantum control methods. Since many quantum control methods are very helpful to study the dynamics of a quantum system and optimize the quantum evolution against imperfections, exploiting these methods may benefit the constructions of geometric gates in more complex quantum systems, and further promote the gate fidelities. This point motivates researches to find approaches for reducing the constrained conditions of NHQC, so that the geometric quantum computation can be more compatible with most of quantum control methods.

Recently, a flexible scheme [51] has been proposed, whose framework is based on a set of vectors, which demand looser restrictions relative to the solutions of the Schrödinger equation used in NHQC. With the relaxation of the conditions, the

*xia-208@163.com

nonadiabatic geometric gates can be constructed in an extensible way with the method of the scheme [51], and the method is called as the NHQC+ because it can collaborate with many quantum control methods including counteradiabatic driving (CD) [52–54], dynamical decoupling (DD) [55–57], single-shot-shaped pulse (SSSP) [58,59], etc., becoming the compound such as NHQC + CD, NHQC + DD, NHQC + SSSP, and so forth. The flexibility of the NHQC+ greatly diversifies the choices of the control parameters. This inspires us to consider whether the NHQC+ can work together with more quantum control methods.

Among many quantum control methods, the reverse engineering [60–65] is a very flexible one, which can cooperate with many useful mathematical tools including the Lie algebra and Lie transforms [66–70], geometric rotation [71,72], quaternion [72,73], and so on. To date, the reverse engineering has shown many interesting applications in investigating and controlling the evolutions of quantum states in multilevel and multiparticle systems [74–76]. However, the combinations of the reverse engineering and the NHQC+ have not been discussed. In fact, the reverse engineering holds the potential in constructing multiple evolution paths for the quantum computation. Considering the fact that many previous NHQC schemes work with time-independent eigenvectors of the Hamiltonian, some control parameters of the Hamiltonian should not vary with time, and the realizations of the quantum gates usually require one or more auxiliary energy levels [77]. The exploitations of multiple evolution paths can give more degrees of freedom to the control parameters, which allow the nonadiabatic geometric gates to be constructed without the auxiliary levels. Moreover, different geometric phases acquired in different evolution paths can enrich the types of available quantum gates. Hence, the study of the combination of the reverse engineering and the NHQC+ may make the implementations of nonadiabatic geometric quantum gates even more flexible.

In this paper, as an attempt for the combination of the reverse engineering and the NHQC+, we study the implementations of nonadiabatic geometric quantum gates with the invariant based reverse engineering (IBRE) and NHQC+. We first show the IBRE method can provide multiple evolution paths, which satisfying all of the conditions of the NHQC+. Thus, we can build up a compound, read as NHQC + IBRE, for the multipath quantum computation. The scheme shares the flexibility of the IBRE, and can benefit the implementation of geometric quantum gate in many ways. First, all of vectors in the computational basis can be covered by multiple evolution paths, so that the requirement of the auxiliary levels can be avoided. Second, the scheme allows most of the control parameters to vary in a cycling evolution. Based on the variation of parameters, different geometric phases can be acquired in different evolution paths. With the acquired geometric phases, we can realize multiple types of nonadiabatic geometric quantum gates by only adjusting the boundary conditions of control parameters. Third, the scheme can be applied in various physical systems with different dynamic invariants constructed by the Lie algebra. To demonstrate the application of the scheme, we discuss the implementations of nontrivial two-qubit nonadiabatic geometric quantum gates of spin qubits in a double-quantum-dot system [78,79], where two spins can be

individually driven by magnetic fields and couple with each other through the Heisenberg interaction. The performance of the scheme is estimated with the numerical simulations, and the results indicate the scheme holds robustness against the errors and noise. Therefore, we hope the scheme can be helpful to the fast and precise implementation of geometric quantum computations.

The article is organized as follows. In Sec. II, we briefly review the Lewis-Riesenfeld invariant theory [80] and the method for constructing dynamic invariant with the help of Lie algebra [67]. In Sec. III, we introduce the conditions of the NHQC+ [51] and show the construction of the NHQC + IBRE. In Sec. IV, we discuss the physical implementations of nonadiabatic geometric quantum gates of two coupled spins in a double-quantum-dot system with the NHQC + IBRE as an application of the scheme. In Sec. V, we analyze the performance of the quantum gates with the NHQC + IBRE under the influence of the errors and noise via numerical simulations. Finally, the conclusion is given in Sec. IV.

II. REVIEW OF INVARIANT BASED REVERSE ENGINEERING

A. Lewis-Riesenfeld invariant theory

We now briefly review the Lewis-Riesenfeld invariant theory [80]. Let us consider a system with Hamiltonian $H(t)$. By introducing a Hermitian invariant operator $I(t)$, which satisfies ($\hbar = 1$)

$$i \frac{\partial}{\partial t} I(t) - [H(t), I(t)] = 0, \quad (1)$$

the solution $|\psi(t)\rangle$ of the time-dependent Schrödinger equation

$$i \frac{\partial}{\partial t} |\psi(t)\rangle = H(t) |\psi(t)\rangle \quad (2)$$

can be expanded by eigenvectors of $I(t)$ as

$$|\psi(t)\rangle = \sum_k C_k e^{i\alpha_k(t)} |\phi_k(t)\rangle. \quad (3)$$

Here, $|\phi_k(t)\rangle$ is the k th eigenvector of $I(t)$, $C_k = \langle \phi_k(0) | \psi(0) \rangle$ is the corresponding coefficient, and $\alpha_k(t)$ is the Lewis-Riesenfeld phase for $|\phi_k(t)\rangle$. Assuming the initial time is $t_i = 0$, $\alpha_k(t)$ reads as

$$\alpha_k(t) = \int_0^t \langle \phi_k(t') | i \frac{\partial}{\partial t'} - H(t') | \phi_k(t') \rangle dt'. \quad (4)$$

B. Constructing dynamic invariants with Lie algebra

In this section, we review the method for the constructing of invariants with Lie algebra [67]. Consider a system whose Hamiltonian is $H(t)$. We suppose that $H(t)$ could be described by

$$H(t) = \sum_{j=1}^N \lambda_j(t) G_j, \quad (5)$$

with $\{G_j\}$ being a set of Hermitian generators spanning a Lie algebra (dynamical algebra [81]), which satisfies the

orthogonal condition with the Hilbert-Schmidt inner product $(X_1, X_2) = \text{Tr}(X_1 X_2^\dagger)$. Assuming

$$[G_j, G_{j'}] = i \sum_J \mu_{jj'} G_J \quad (j, j', J \in \{1, 2, 3, \dots, N\}), \quad (6)$$

if an invariant $I(t)$ of the system could be written by

$$I(t) = \sum_{j=1}^N \xi_j(t) G_j, \quad (7)$$

we have

$$\dot{\xi}_j(t) = \sum_{j,j'=1}^N \lambda_j(t) \xi_{j'}(t) \mu_{jj'}, \quad (8)$$

when combining Eq. (1) and Eqs. (5)–(7).

As the existence of invariant in the form as Eq. (7) is very important for the construction of the invariant, we first prove that when $\{\lambda_j(t)\}$ are given, one can obtain solutions of $\{\xi_l(t)\}$ from Eq. (8). Thus, we define an $N \times N$ matrix $\mathcal{P}(t)$ with matrix element

$$\mathcal{P}_{j'j}(t) = \sum_{j=1}^N \lambda_j(t) \mu_{jj'}, \quad (9)$$

and an N -dimension vector

$$\vec{\xi}(t) = \begin{bmatrix} \xi_1(t) \\ \xi_2(t) \\ \dots \\ \xi_N(t) \end{bmatrix}, \quad (10)$$

such that Eq. (8) can be rewritten as

$$\dot{\vec{\xi}}(t) = \mathcal{P}(t) \vec{\xi}(t). \quad (11)$$

Equation (11) describes first-order linear differential equations. According to the existence theorem of solutions for first-order linear differential equations [82], one can find a solution for $\vec{\xi}(t)$ theoretically. Thus, there exists an invariant in the form of Eq. (7).

Based on the results above, one can always find an invariant from the differential equations shown in Eq. (11) with a given set of $\{\lambda_j(t)\}$, theoretically. However, the process of solving the invariant $I(t)$ in Eq. (7) is usually very complex. Thus, rather than solving the invariant $I(t)$ with known $\{\lambda_j(t)\}$, reversely constructing control Hamiltonian of the system with parameters $\{\xi_j(t)\}$ of the invariant is a good idea in some cases. For this sake, an $N \times N$ matrix $\mathcal{M}(t)$ with matrix element and an N -dimension vector are defined as

$$\mathcal{M}_{jj}(t) = \sum_{j'=1}^N \xi_{j'}(t) \mu_{jj'} \quad (12)$$

and

$$\vec{\lambda}(t) = \begin{bmatrix} \lambda_1(t) \\ \lambda_2(t) \\ \dots \\ \lambda_N(t) \end{bmatrix}. \quad (13)$$

Then, Eq. (8) can be rewritten as

$$\dot{\vec{\xi}}(t) = \mathcal{M}(t) \vec{\lambda}(t). \quad (14)$$

Reversely solving $\vec{\lambda}(t)$ from Eq. (14), one can design the control Hamiltonian by design $\vec{\xi}(t)$ and $\vec{\lambda}(t)$, with the question about solving a set of complex differential equations being avoided. We show in Appendices D and E that the matrix $\mathcal{M}(t)$ is always not a full-rank matrix, and Eq. (14) can be solved with constraint equations.

III. COMBINATION OF THE NHQC+ AND THE IBRE

A. Conditions of the NHQC+

In this section, to make the combination of the NHQC+ and the IBRE more clear, we briefly review the conditions of the NHQC+ [51]. We consider a complete basis $\mathcal{V} = \{|\psi_m(t)\rangle | m = 1, 2, \dots, M\}$, in which all the vectors follow the Schrödinger equation. Besides, there exists a subspace \mathcal{S}_1 spanned by the vectors in the subset \mathcal{V}_1 of \mathcal{V} . Generally speaking, to realize the NHQC in \mathcal{S}_1 , two conditions should be satisfied [36,37]:

$$(i) \sum_{|\psi_m\rangle \in \mathcal{V}_1} |\psi_m(T)\rangle \langle \psi_m(T)| = \sum_{|\psi_m\rangle \in \mathcal{V}_1} |\psi_m(0)\rangle \langle \psi_m(0)|, \quad (15)$$

$$(ii) \langle \psi_m(t) | H(t) | \psi_{m'}(t) \rangle = 0, \quad (|\psi_m\rangle, |\psi_{m'}\rangle \in \mathcal{V}_1), \quad (16)$$

which ensure a cyclic evolution without dynamic phases being accumulated during the time interval $[0, T]$. Since the condition shown in Eq. (16) requires constraints for all $|\psi_m\rangle, |\psi_{m'}\rangle \in \mathcal{V}_1$, the evolution may sometimes be relatively complex to be combined with some pulse design methods and optimization methods. To remove some of the constraints, the NHQC+ suggests to find an alternative basis as $\tilde{\mathcal{V}} = \{|\tilde{\psi}_m(t)\rangle | m = 1, 2, \dots, M\}$, in which $|\tilde{\psi}_m(t)\rangle$ is connected with $|\psi_m(t)\rangle$ at the initial and the final time as $|\tilde{\psi}_m(T)\rangle = |\tilde{\psi}_m(0)\rangle = |\psi_m(0)\rangle$. According to the results of Ref. [51], to construct a nonadiabatic geometric quantum gate with NHQC+, the vectors in $\tilde{\mathcal{V}}$ should satisfy several conditions. First, defining $\Xi_m(t) = |\tilde{\psi}_m(t)\rangle \langle \tilde{\psi}_m(t)|$, $\Xi_m(t)$ should satisfy the von Neumann equation

$$\frac{d}{dt} \Xi_m(t) = -i[H(t), \Xi_m(t)]. \quad (17)$$

Besides, for each $|\tilde{\psi}_m(t)\rangle \in \tilde{\mathcal{V}}$, the condition in the following should be fulfilled:

$$\vartheta_m(T) = - \int_0^T \langle \tilde{\psi}_m(t) | H(t) | \tilde{\psi}_m(t) \rangle dt = 0, \quad (18)$$

to make the dynamic phase $\vartheta_m(T)$ acquired in the whole process vanish, such that the evolution becomes purely geometric as

$$U(T, 0) = \sum_m e^{i\Theta_m(T)} |\tilde{\psi}_m(0)\rangle \langle \tilde{\psi}_m(0)|, \quad (19)$$

with

$$\Theta_m(t) = i \int_0^t \langle \tilde{\psi}_m(t') | \dot{\tilde{\psi}}_m(t') \rangle dt'. \quad (20)$$

Comparing the condition shown in Eq. (18) with that shown in Eq. (16), the constraints for $m \neq m'$ are removed. Moreover, the condition shown in Eq. (16) should be satisfied at each moment, while the condition shown in Eq. (18) is only relative to the integral in the time interval $[0, T]$. Thus, the NHQC+

may be compatible with different pulse design methods and optimization methods.

B. NHQC + IBRE for multipath nonadiabatic geometric quantum computation

Here, we show that the IBRE is compatible with the NHQC+, thus, IBRE can be integrated with NHQC+ and become a compound, the NHQC + IBRE. First, we assume that the eigenvectors $\{|\phi_\ell(t)\rangle\}$ of a dynamic invariant $I(t)$ form a complete and normal orthogonal basis of a Hilbert space.

Thus, when adjusting the initial values of the parameters in eigenvectors $\{|\phi_\ell(t)\rangle\}$, any complete and orthogonal set formed by the solutions of the Schrödinger equation can be connected with $\{|\phi_\ell(t)\rangle\}$ at the initial and the final time of a cycling evolution. As $|\phi_\ell(t)\rangle$ is the eigenvector of the dynamic invariant $I(t)$, exploiting Eq. (1), we can derive

$$i(\varepsilon_\ell - \varepsilon_{\ell'})\langle\phi_{\ell'}(t)|\dot{\phi}_\ell(t)\rangle = (\varepsilon_\ell - \varepsilon_{\ell'})\langle\phi_{\ell'}(t)|H(t)|\phi_\ell(t)\rangle, \quad (21)$$

where the result $\langle\dot{\phi}_{\ell'}(t)|\phi_\ell(t)\rangle + \langle\phi_{\ell'}(t)|\dot{\phi}_\ell(t)\rangle = 0$ is used. For $\varepsilon_{\ell'} \neq \varepsilon_\ell$, we have

$$\begin{aligned} \langle\phi_{\ell'}(t)|\dot{\phi}_\ell(t)\rangle + i\langle\phi_{\ell'}(t)|H(t)|\phi_\ell(t)\rangle &= 0 \\ \Rightarrow |\phi_{\ell'}(t)\rangle\langle\phi_{\ell'}(t)|\dot{\phi}_\ell(t)\rangle\langle\phi_\ell(t)| + i|\phi_{\ell'}(t)\rangle\langle\phi_{\ell'}(t)|H(t)|\phi_\ell(t)\rangle\langle\phi_\ell(t)| &= 0 \\ \Rightarrow \sum_{\ell' \neq \ell} |\phi_{\ell'}(t)\rangle\langle\phi_{\ell'}(t)|\dot{\phi}_\ell(t)\rangle\langle\phi_\ell(t)| + i|\phi_{\ell'}(t)\rangle\langle\phi_{\ell'}(t)|H(t)|\phi_\ell(t)\rangle\langle\phi_\ell(t)| &= 0 \\ \Rightarrow \sum_{\ell' \neq \ell} |\phi_{\ell'}(t)\rangle\langle\phi_{\ell'}(t)|[\dot{\phi}_\ell(t)\rangle\langle\phi_\ell(t)| + iH(t)\tilde{\Xi}_\ell(t)] &= 0, \end{aligned} \quad (22)$$

with $\tilde{\Xi}_\ell(t) = |\phi_\ell(t)\rangle\langle\phi_\ell(t)|$. Assuming that $|\phi_\ell(t)\rangle$ is a nondegenerate eigenvector of the dynamic invariant, one can further obtain

$$|\dot{\phi}_\ell(t)\rangle\langle\phi_\ell(t)| + iH(t)\tilde{\Xi}_\ell(t) = |\phi_\ell(t)\rangle\langle\phi_\ell(t)|[\dot{\phi}_\ell(t)\rangle\langle\phi_\ell(t)| + iH(t)\tilde{\Xi}_\ell(t)], \quad (23)$$

based on the completeness of basis $\{|\phi_\ell(t)\rangle\}$. From Eq. (23), the following results can be derived:

$$\begin{aligned} |\dot{\phi}_\ell(t)\rangle\langle\phi_\ell(t)| + iH(t)\tilde{\Xi}_\ell(t) &= \langle\phi_\ell(t)|\dot{\phi}_\ell(t)\rangle\tilde{\Xi}_\ell(t) + i\tilde{\Xi}_\ell(t)H(t)\tilde{\Xi}_\ell(t), \\ \langle\phi_\ell(t)|\dot{\phi}_\ell(t)\rangle - i\tilde{\Xi}_\ell(t)H(t) &= \langle\dot{\phi}_\ell(t)|\phi_\ell(t)\rangle\tilde{\Xi}_\ell(t) - i\tilde{\Xi}_\ell(t)H(t)\tilde{\Xi}_\ell(t). \end{aligned} \quad (24)$$

Adding the two equations in Eq. (24) together, we finally derive

$$\frac{d}{dt}\tilde{\Xi}_\ell(t) = -i[H(t), \tilde{\Xi}_\ell(t)], \quad (25)$$

under the condition $\langle\dot{\phi}_\ell(t)|\phi_\ell(t)\rangle + \langle\phi_\ell(t)|\dot{\phi}_\ell(t)\rangle = 0$. Until now, we have shown the nondegenerate eigenvectors of the dynamic invariant $I(t)$ satisfy the von Neumann equation shown in Eq. (17). However, for two arbitrary degenerate eigenvectors $|\phi_{\ell_1}(t)\rangle$ and $|\phi_{\ell_2}(t)\rangle$, the satisfactions of von Neumann equation could not be ensured since $\varepsilon_{\ell_1} = \varepsilon_{\ell_2}$.

To ensure the satisfactions of the von Neumann equation with degenerate eigenvectors, we consider the superpositions of the degenerate eigenvectors. As an example, we assume there exist only two degenerate eigenvectors $|\phi_{\ell_1}(t)\rangle$ and $|\phi_{\ell_2}(t)\rangle$. Introducing a set of operators as $\tilde{\Xi}'_\ell(t) = |\tilde{\phi}_\ell(t)\rangle\langle\tilde{\phi}_\ell(t)|$ with

$$\begin{aligned} |\tilde{\phi}_{\ell_1}(t)\rangle &= \cos[\beta_1(t)]|\phi_1(t)\rangle + e^{i\beta_2(t)}\sin[\beta_1(t)]|\phi_2(t)\rangle, \\ |\tilde{\phi}_{\ell_2}(t)\rangle &= \sin[\beta_1(t)]|\phi_1(t)\rangle - e^{i\beta_2(t)}\cos[\beta_1(t)]|\phi_2(t)\rangle, \\ |\tilde{\phi}_\ell(t)\rangle &= |\phi_\ell(t)\rangle \quad (\ell \neq \ell_1, \ell_2), \end{aligned} \quad (26)$$

the vectors $\{|\tilde{\phi}_\ell(t)\rangle\}$ also form a complete and normal orthogonal basis of the Hilbert space. Then, we substitute $\tilde{\Xi}'_{\ell_1}(t)$ and $\tilde{\Xi}'_{\ell_2}(t)$ into the von Neumann equation in Eq. (17). After that, the values of $\beta_1(t)$, $\beta_2(t)$ can be reversely solved to make all of the redefined operators $\{\tilde{\Xi}'_\ell(t)\}$ fulfill the von Neumann equation in Eq. (17). For the cases with more than two degenerate eigenvectors, we just need to consider the

superpositions of all the degenerate eigenvectors with the same eigenvalues and construct a serial of redefined operators $\{\tilde{\Xi}'_\ell(t)\}$. In this way, one can always obtain a set of eigenvectors $\{|\tilde{\phi}_\ell(t)\rangle\}$ of dynamic invariant $I(t)$ with all of the operators $\{\tilde{\Xi}'_\ell(t)\}$ satisfying the von Neumann equation in Eq. (17) (see Appendix B for details).

Now according to the condition in Eq. (18), one thing remained is to make the Lewis-Riesenfeld phase shown in Eq. (4) purely geometric. Thus, we calculate the Lewis-Riesenfeld $\tilde{\alpha}_\ell(T) = \tilde{\vartheta}_\ell(T) + \tilde{\Theta}_\ell(T)$ with the dynamic part $\tilde{\vartheta}_\ell(T)$ and the geometric part $\tilde{\Theta}_\ell(T)$ acquired by $|\tilde{\phi}_\ell(t)\rangle$ in a cycling evolution as

$$\tilde{\vartheta}_\ell(T) = -\int_0^T \langle\tilde{\phi}_\ell(t')|H(t')|\tilde{\phi}_\ell(t')\rangle dt' \quad (27)$$

and

$$\tilde{\Theta}_\ell(T) = i\int_0^T \langle\tilde{\phi}_\ell(t')|\dot{\tilde{\phi}}_\ell(t')\rangle dt'. \quad (28)$$

Hence, the condition in Eq. (18) is converted to $\tilde{\vartheta}_\ell(T) = 0$.

To sum up the discussions in this section, we have first shown the approach to find a set of eigenvectors $\{|\tilde{\phi}_\ell(t)\rangle\}$ of dynamic invariant $I(t)$ satisfying the von Neumann equation in Eq. (17). Consequently, the selections of the vectors for NHQC+ are naturally completed by the IBRE, and the core of the construction of NHQC + IBRE is selecting proper control parameters to make $\tilde{\vartheta}_\ell(T) = 0$. As a dynamic invariant $I(t)$ can be parametrized in a flexible way relating to the number

of the generators in the dynamical algebra, the dynamic phases can be flexibly eliminated. Moreover, because all of the eigenvectors $\{|\hat{\phi}_\ell(t)\rangle\}$ of the dynamic invariant $I(t)$ can vary with the control parameters and acquired different geometric phases during the evolutions, exploiting them as the evolution paths, we can realize multipath nonadiabatic geometric quantum computation based on the NHQC + IBRE.

IV. PHYSICAL IMPLEMENTATION OF THE NONADIABATIC GEOMETRIC QUANTUM GATES WITH NHQC + IBRE

In this section, let us discuss the applications of the NHQC + IBRE. The major example considered here is the realization of nontrivial two-qubit nonadiabatic geometric quantum gates in a double-quantum-dot system. The NHQC + IBRE can also be used to realize arbitrary single-qubit nonadiabatic geometric quantum gates, which are shown in Appendix A.

A. Hamiltonian of two coupled spins in a double-quantum-dot system

We consider a double-quantum-dot system with two spin qubits l and r confined in the left and right quantum dots, respectively. The spins l and r are individually driven

$$H(t) = \frac{1}{2} \begin{bmatrix} 0 & gB_{rx}(t) - igB_{ry}(t) & gB_{lx}(t) - igB_{ly}(t) & 0 \\ gB_{rx}(t) + igB_{ry}(t) & -2B_{rz}(t) - J_z(t) & J(t) & gB_{lx}(t) - igB_{ly}(t) \\ gB_{lx}(t) + igB_{ly}(t) & J(t) & -2B_{lz}(t) - J_z(t) & gB_{rx}(t) - igB_{ry}(t) \\ 0 & gB_{lx}(t) + igB_{ly}(t) & gB_{rx}(t) - igB_{ry}(t) & -2B_{lz}(t) - 2B_{rz}(t) \end{bmatrix} + \frac{2B_{lz}(t) + 2B_{rz}(t) + J(t)}{4}, \quad (30)$$

where the last term could be dropped as it only produces a global phase.

B. Construction of the dynamic invariant

To simplify construction of the dynamic invariant based on the Hamiltonian in Eq. (30), we set

$$\begin{aligned} B_{lx}(t) &= -\sum_{\iota=1,2} B_\iota(t) \sin \omega_\iota t, & B_{ly}(t) &= \sum_{\iota=1,2} B_\iota(t) \cos \omega_\iota t, \\ B_{rx}(t) &= \sum_{\iota=1,2} B_r(t) \cos \omega_r t, & B_{ry}(t) &= \sum_{\iota=1,2} B_r(t) \sin \omega_r t, \\ B_{lz}(t) &= B_{rz}(t) = B_z(t), & \Delta_1(t) &= -B_z(t) - J_z(t)/2, \\ \Delta_2(t) &= -2B_z(t). \end{aligned} \quad (31)$$

Here, $\Delta_1(t)$ and $\Delta_2(t)$ are both considered to be time independent and satisfy the conditions as

$$\omega_{l1} = \omega_{r1} = -\Delta_1, \quad \omega_{l2} = \omega_{r2} = \Delta_1 - \Delta_2. \quad (32)$$

Under the condition $|gB_l(t)|, |gB_r(t)| \ll |2\Delta_1 - \Delta_2|$, the rapidly oscillating terms are discarded in the rotation frame

by magnetic fields $\vec{B}_l(t) = B_{lx}(t)\vec{e}_x + B_{ly}(t)\vec{e}_y + B_{lz}(t)\vec{e}_z$, $\vec{B}_r(t) = B_{rx}(t)\vec{e}_x + B_{ry}(t)\vec{e}_y + B_{rz}(t)\vec{e}_z$, with \vec{e}_x , \vec{e}_y , and \vec{e}_z being the unit vector along x , y , and z axis, respectively. In addition, the spins l and r can couple with each other through the Heisenberg interactions. The Hamiltonian of the system is described by [78,79]

$$H(t) = g\vec{B}_l(t) \cdot \vec{S}_l + g\vec{B}_r(t) \cdot \vec{S}_r + J_x(t)S_{lx}S_{rx} + J_y(t)S_{ly}S_{ry} + J_z(t)S_{lz}S_{rz}, \quad (29)$$

where g is the gyromagnetic ratio, and $\vec{S}_l = S_{lx}\vec{e}_x + S_{ly}\vec{e}_y + S_{lz}\vec{e}_z$, $\vec{S}_r = S_{rx}\vec{e}_x + S_{ry}\vec{e}_y + S_{rz}\vec{e}_z$ are the spin operators of the spins l and r . Besides, $J_x(t)$, $J_y(t)$, and $J_z(t)$ are the strengths of Heisenberg interactions in x , y , and z directions, respectively. As shown by the previous schemes that [78,79,83,84], the Heisenberg interactions used here can be induced by the exchange interaction between spins. The strength of the coupling can be adjusted with fast gate voltage control of a gate between left and right quantum dots. The speed of the control of the exchange coupling is in the order of ns to ms, which allows fast gate implementations [78]. Moreover, the experiment devices in Ref. [78] can provide exquisite control of single electrons and nearest-neighbor exchange coupling, with the potential to scale to at least nine dots in a linear array. Here, we assume that $J_x(t) = J_y(t) = J(t)$ such that in the basis $\{|\uparrow\uparrow\rangle, |\uparrow\downarrow\rangle, |\downarrow\uparrow\rangle, |\downarrow\downarrow\rangle\}$, the matrix form of the Hamiltonian in Eq. (29) is

of $R(t) = e^{-iH_0 t}$ with

$$H_0 = \Delta_1(|\uparrow\downarrow\rangle\langle\uparrow\downarrow| + |\downarrow\uparrow\rangle\langle\downarrow\uparrow|) + \Delta_2|\downarrow\downarrow\rangle\langle\downarrow\downarrow|, \quad (33)$$

such that the effective Hamiltonian $H_e(t)$ of the system in the rotating frame can be described in the $\mathfrak{so}(4)$ algebra [which is isomorphic to the standard $\mathfrak{so}(4)$ Lie algebra, see Appendix C for details] spanned by

$$\begin{aligned} G_1 &= \begin{bmatrix} 0 & 1 & 0 & 0 \\ 1 & 0 & 0 & 0 \\ 0 & 0 & 0 & 0 \\ 0 & 0 & 0 & 0 \end{bmatrix}, & G_2 &= \begin{bmatrix} 0 & 0 & 0 & 0 \\ 0 & 0 & 0 & 0 \\ 0 & 0 & 0 & 1 \\ 0 & 0 & 1 & 0 \end{bmatrix}, \\ G_3 &= \begin{bmatrix} 0 & 0 & 0 & 0 \\ 0 & 0 & 1 & 0 \\ 0 & 1 & 0 & 0 \\ 0 & 0 & 0 & 0 \end{bmatrix}, & G_4 &= \begin{bmatrix} 0 & 0 & 0 & 1 \\ 0 & 0 & 0 & 0 \\ 0 & 0 & 0 & 0 \\ 1 & 0 & 0 & 0 \end{bmatrix}, \\ G_5 &= \begin{bmatrix} 0 & 0 & -i & 0 \\ 0 & 0 & 0 & 0 \\ i & 0 & 0 & 0 \\ 0 & 0 & 0 & 0 \end{bmatrix}, & G_6 &= \begin{bmatrix} 0 & 0 & 0 & 0 \\ 0 & 0 & 0 & -i \\ 0 & 0 & 0 & 0 \\ 0 & i & 0 & 0 \end{bmatrix}, \end{aligned} \quad (34)$$

as

$$H_e(t) = [gB_{r_1}(t)G_1 + gB_{r_2}(t)G_2 + J(t)G_3 + gB_{l_1}(t)G_5 + gB_{l_2}(t)G_6]/2. \tag{35}$$

Now, let us begin to find a dynamic invariant of the evolution with Lie algebra. First, according to Eq. (7), the invariant is assumed to be

$$I(t) = \sum_{j=1}^6 \xi_j(t)G_j. \tag{36}$$

Then, by using Eq. (14), one can derive

$$\begin{aligned} 2\dot{\xi}_1 &= -gB_{l_1}\xi_3 - gB_{l_2}\xi_4 + J\xi_5, \\ 2\dot{\xi}_2 &= gB_{l_2}\xi_3 + gB_{l_1}\xi_4 - J\xi_6, \\ 2\dot{\xi}_3 &= gB_{l_1}\xi_1 - gB_{l_2}\xi_2 - gB_{r_1}\xi_5 + gB_{r_2}\xi_6, \\ 2\dot{\xi}_4 &= gB_{l_2}\xi_1 - gB_{l_1}\xi_2 + gB_{r_2}\xi_5 - gB_{r_1}\xi_6, \\ 2\dot{\xi}_5 &= -J\xi_1 + gB_{r_1}\xi_3 - gB_{r_2}\xi_4, \end{aligned} \tag{37}$$

$$2\dot{\xi}_6 = J\xi_2 - gB_{r_2}\xi_3 + gB_{r_1}\xi_4.$$

According to Eq. (37), the matrix form of $\mathcal{M}(t)$ in Eq. (14) can be obtained as

$$\mathcal{M}(t) = \frac{1}{2} \begin{bmatrix} 0 & 0 & \xi_5 & -\xi_6 & -\xi_3 & -\xi_4 \\ 0 & 0 & -\xi_6 & -\xi_5 & \xi_4 & \xi_3 \\ -\xi_5 & \xi_6 & 0 & 0 & \xi_1 & -\xi_2 \\ -\xi_6 & \xi_5 & 0 & 0 & -\xi_2 & \xi_1 \\ \xi_3 & -\xi_4 & -\xi_1 & \xi_2 & 0 & 0 \\ \xi_4 & -\xi_3 & \xi_2 & -\xi_1 & 0 & 0 \end{bmatrix}. \tag{38}$$

Since the rank of matrix $\mathcal{M}(t)$ is $\text{rank}[\mathcal{M}(t)] = 4$, two constraint equations for $\{\xi_j(t)|j = 1, 2, 3, 4, 5, 6\}$ can be found as

$$\begin{aligned} (\xi_1 - \xi_2)^2 + (\xi_3 + \xi_4)^2 + (\xi_5 + \xi_6)^2 &= C_1^2, \\ (\xi_1 + \xi_2)^2 + (\xi_3 - \xi_4)^2 + (\xi_5 - \xi_6)^2 &= C_2^2, \end{aligned} \tag{39}$$

from Eq. (37) with C_1 and C_2 being two real constants. As one way to parametrize $\{\xi_j(t)\}$, we suppose $C_1 = C_2 = 1$ and

$$\begin{aligned} \xi_1 &= \cos \theta \cos \eta, & \xi_2 &= -\sin \theta \sin \eta, & \xi_3 &= \sin \theta \cos \eta \sin \varphi, \\ \xi_4 &= -\cos \theta \sin \eta \sin \varphi, & \xi_5 &= \sin \theta \cos \eta \cos \varphi, & \xi_6 &= -\cos \theta \sin \eta \cos \varphi. \end{aligned} \tag{40}$$

Then, by substituting the parametrization of Eq. (40) into Eq. (14), the expressions of the control parameters are derived as

$$\begin{aligned} gB_{l_1}(t) &= (J \cos \varphi + 2\dot{\theta}) \csc \varphi, & gB_{l_2}(t) &= -2\dot{\eta} \csc \varphi, \\ gB_{r_1}(t) &= -2\dot{\varphi} - \frac{2\dot{\eta} \sin 2\eta \cot \varphi - (J + 2\dot{\theta} \cos \varphi) \sin 2\theta \csc \varphi}{\cos 2\eta - \cos 2\theta}, \\ gB_{r_2}(t) &= \frac{2\dot{\eta} \sin 2\theta \cot \varphi - (J + 2\dot{\theta} \cos \varphi) \sin 2\eta \csc \varphi}{\cos 2\eta - \cos 2\theta}. \end{aligned} \tag{41}$$

In addition, the eigenvectors corresponding to the eigenvalues $\varepsilon_1 = 0$, $\varepsilon_2 = 0$, $\varepsilon_3 = 1$, and $\varepsilon_4 = -1$ of the dynamic invariant are

$$\begin{aligned} |\phi_1(t)\rangle &= \begin{bmatrix} i \cos \varphi \sin \eta \\ -\sin \varphi \sin \eta \\ 0 \\ -\cos \eta \end{bmatrix}, & |\phi_2(t)\rangle &= \begin{bmatrix} -\sin \theta \sin \varphi \\ i \sin \theta \cos \varphi \\ \cos \theta \\ 0 \end{bmatrix}, \\ |\phi_3(t)\rangle &= \frac{1}{\sqrt{2}} \begin{bmatrix} -\cos \theta \sin \varphi + i \cos \eta \cos \varphi \\ -\cos \eta \sin \varphi + i \cos \theta \cos \varphi \\ -\sin \theta \\ \sin \eta \end{bmatrix}, & |\phi_4(t)\rangle &= \frac{1}{\sqrt{2}} \begin{bmatrix} \cos \theta \sin \varphi + i \cos \eta \cos \varphi \\ -\cos \eta \sin \varphi - i \cos \theta \cos \varphi \\ \sin \theta \\ \sin \eta \end{bmatrix}, \end{aligned} \tag{42}$$

respectively. Since the eigenvectors $|\phi_1(t)\rangle$ and $|\phi_2(t)\rangle$ are degenerate, we use the suppositions shown in Eq. (26) to find another set of eigenvectors $\{|\tilde{\phi}_\ell(t)\rangle| \ell = 1, 2, 3, 4\}$. Based on the von Neumann equation, $\beta_1(t) = \pi/4$ and $\beta_2(t) = 0$ are derived. Moreover, the time derivatives of the dynamic phases and geometric phases acquired by $|\tilde{\phi}_\ell(t)\rangle$ are calculated as

$$\begin{aligned} \dot{\vartheta}_1(t) &= \frac{(J + 2\dot{\theta} \cos \varphi) \sin \eta \cos \theta \csc \varphi - 2\dot{\eta} \cos \eta \sin \theta \cot \varphi}{\cos 2\eta - \cos 2\theta} - \dot{\varphi} \sin \eta \sin \theta, \\ \dot{\vartheta}_2(t) &= \frac{2\dot{\eta} \cos \eta \sin \theta \cot \varphi - (J + 2\dot{\theta} \cos \varphi) \sin \eta \cos \theta \csc \varphi}{\cos 2\eta - \cos 2\theta} + \dot{\varphi} \sin \eta \sin \theta, \\ \dot{\vartheta}_3(t) &= \frac{2\dot{\eta} \sin \eta \cos \theta \cot \varphi - (J + 2\dot{\theta} \cos \varphi) \cos \eta \sin \theta \csc \varphi}{\cos 2\eta - \cos 2\theta} + \dot{\varphi} \cos \eta \cos \theta, \\ \dot{\vartheta}_4(t) &= \frac{(J + 2\dot{\theta} \cos \varphi) \cos \eta \sin \theta \csc \varphi - 2\dot{\eta} \sin \eta \cos \theta \cot \varphi}{\cos 2\eta - \cos 2\theta} - \dot{\varphi} \cos \eta \cos \theta, \end{aligned} \tag{43}$$

and

$$\begin{aligned}\dot{\tilde{\Theta}}_1(t) &= \dot{\varphi} \sin \theta \sin \eta, & \dot{\tilde{\Theta}}_2(t) &= -\dot{\varphi} \sin \theta \sin \eta, \\ \dot{\tilde{\Theta}}_3(t) &= -\dot{\varphi} \cos \theta \cos \eta, & \dot{\tilde{\Theta}}_4(t) &= \dot{\varphi} \cos \theta \cos \eta.\end{aligned}\quad (44)$$

Based on the results of Eqs. (43) and (44), we can further design control parameters for the elimination of the dynamic phases and the acquisition of different geometric phases.

C. Implementations of two-qubit nonadiabatic geometric quantum gates with NHQC + IBRE

Let us now demonstrate the construction of nontrivial two-qubit nonadiabatic geometric quantum gate with NHQC + IBRE. We consider a process that the geometric phases acquired after an interaction time T are $\tilde{\Theta}_1(T) = \tilde{\Theta}_2(T) = 0$, $\tilde{\Theta}_3(T) = -\tilde{\Theta}_4(T) = -\pi$, and the dynamic phases acquired in the process are all zero. Moreover, all of the parameters $\theta(t)$, $\eta(t)$, and $\varphi(t)$ vary along loops, i.e., $\theta(0) = \theta(T) + 2\kappa_1\pi$, $\eta(0) = \eta(T) + 2\kappa_2\pi$, and $\varphi(0) = \varphi(T) + 2\kappa_3\pi$ (κ_1 , κ_2 , and κ_3 are integers). In this case, the evolution operator $U(t)$ at $t = T$ can be described as

$$\begin{aligned}U(T) &= \sum_{\ell=1}^4 e^{i\tilde{\Theta}_\ell(T)} \tilde{\Xi}'_\ell(T) \\ &= \begin{bmatrix} -\cos 2\eta \cos^2 \varphi - \cos 2\theta \sin^2 \varphi & i(\cos 2\eta - \cos 2\theta) \sin 2\varphi/2 & -\sin 2\theta \sin \varphi & -i \sin 2\eta \cos \varphi \\ -i(\cos 2\eta - \cos 2\theta) \sin 2\varphi/2 & -\cos 2\theta \cos^2 \varphi - \cos 2\eta \sin^2 \varphi & i \sin 2\theta \cos \varphi & \sin 2\eta \sin \varphi \\ -\sin 2\theta \sin \varphi & -i \sin 2\theta \cos \varphi & \cos 2\theta & 0 \\ i \sin 2\eta \cos \varphi & \sin 2\eta \sin \varphi & 0 & \cos 2\eta \end{bmatrix},\end{aligned}\quad (45)$$

where parameters θ , η , and φ take the values of $\theta(T)$, $\eta(T)$, and $\varphi(T)$, respectively. As examples, we investigate the implementations of two types of two-qubit gates. More specifically, when $\eta(T) = 0$, $\theta(T) = \pi/4$, $\varphi(T) = 0$, we can implement a SWAP-like two-qubit gate [85,86] (S gate for short in the following discussions) with the NHQC + IBRE as

$$U_S = \begin{bmatrix} -1 & 0 & 0 & 0 \\ 0 & 0 & i & 0 \\ 0 & -i & 0 & 0 \\ 0 & 0 & 0 & 1 \end{bmatrix}.\quad (46)$$

Besides, for $\eta(T) = 0$, $\theta(T) = \pi/4$, $\varphi(T) = -\pi/2$, a controlled-not-like two-qubit gate (C gate for short in the following discussions)

$$U_C = \begin{bmatrix} 0 & 0 & 1 & 0 \\ 0 & -1 & 0 & 0 \\ 1 & 0 & 0 & 0 \\ 0 & 0 & 0 & 1 \end{bmatrix},\quad (47)$$

with spin r as the controlled qubit can be obtained based on NHQC + IBRE.

Now, let us design the control parameters according to the boundary conditions given above Eqs. (46) and (47) to realize the S gate and the C gate with NHQC + IBRE, respectively. First, we select $\eta(t) = 0$, such that $\dot{\tilde{\vartheta}}_1(t) = \dot{\tilde{\vartheta}}_2(t) = \dot{\tilde{\Theta}}_1(t) = \dot{\tilde{\Theta}}_2(t) = 0$. To make the control parameters vary along loops, we set

$$\begin{aligned}\varphi(t) &= \varphi_0 + \pi \left[1 - \cos \left(\frac{\pi t}{T} \right) \right], \\ \theta(t) &= \frac{\pi}{4} + \Upsilon \sin^2 \left(\frac{\pi t}{T} \right),\end{aligned}\quad (48)$$

where Υ is a time-independent parameter. We set $\varphi_0 = 0$ for the S gate and $\varphi_0 = -\pi/2$ for the C gate. By numerically

calculating Eq. (28), $\Upsilon = 0.3867$ is obtained to fulfill the condition $\tilde{\Theta}_3(T) = -\tilde{\Theta}_4(T) = -\pi$. On the other hand, to eliminate the dynamic phases, we set

$$J(t) = -2\dot{\theta} \cos \varphi + \dot{\varphi} \sin \varphi \sin 2\theta,\quad (49)$$

according to Eq. (43). To estimate the performance of the quantum gates, we exploit a distance between two \mathcal{N} -dimensional unitary operators U_1 and U_2 as

$$d(U_1, U_2) = 1 - |\text{Tr}(U_1 U_2^\dagger)|^2 / \mathcal{N}^2,\quad (50)$$

which describes the upper limit of the average error in the implementations of quantum gates. In Figs. 1(a) and 1(b), we plot the distances $d(U_e(t), U_S)$ and $d(U_e(t), U_C)$ versus t/T , respectively, with $U_e(t)$ being the evolution operator of the system governed by the effective Hamiltonian $H_e(t)$ shown in Eq. (35). According to the red solid lines in Figs. 1(a) and 1(c), both $d(U_e(t), U_S)$ and $d(U_e(t), U_C)$ decrease from 1 to 0 in the time interval $[0, T]$. Thus, the dynamics based on the effective Hamiltonian is valid with the parameters designed in Eq. (48). Besides, $gB_{l_1}(t)$, $gB_{r_1}(t)$, and $J(t)$ versus t/T in the implementations of the S gate and C gate are plotted in Figs. 1(c) and 1(d), respectively. Since we have $gB_{l_2}(t) = gB_{r_2}(t) = 0$ with the selected parameters, $gB_{l_2}(t)$ and $gB_{r_2}(t)$ are not plotted in the Figs. 1(c) and 1(d). According to Figs. 1(c) and 1(d), we have the maximal value Ω_{\max} of control fields as

$$\Omega_{\max} = \max_{t \in [0, T]} \{ |gB_{l_1}(t)|, |gB_{r_1}(t)|, |J(t)| \} \simeq 16.76/T,\quad (51)$$

in both of the implementations of the S gate and the C gate. Furthermore, to compare the evolution $U_e(t)$ of the effective dynamics with the evolution $U(t)$ governed by the original Hamiltonian $H(t)$ in Eq. (29), we also plot the distances $d(U(t), \tilde{U}_S)$ and $d(U(t), \tilde{U}_C)$ versus t/T in Figs. 1(a) and 1(b), respectively. Here, we set $\tilde{U}_S(t) = e^{-iH_0 t} U_S(t)$ and $\tilde{U}_C(t) = e^{-iH_0 t} U_C(t)$, as the implementations of nonadiabatic geometric quantum gates are discussed in the rotating frame

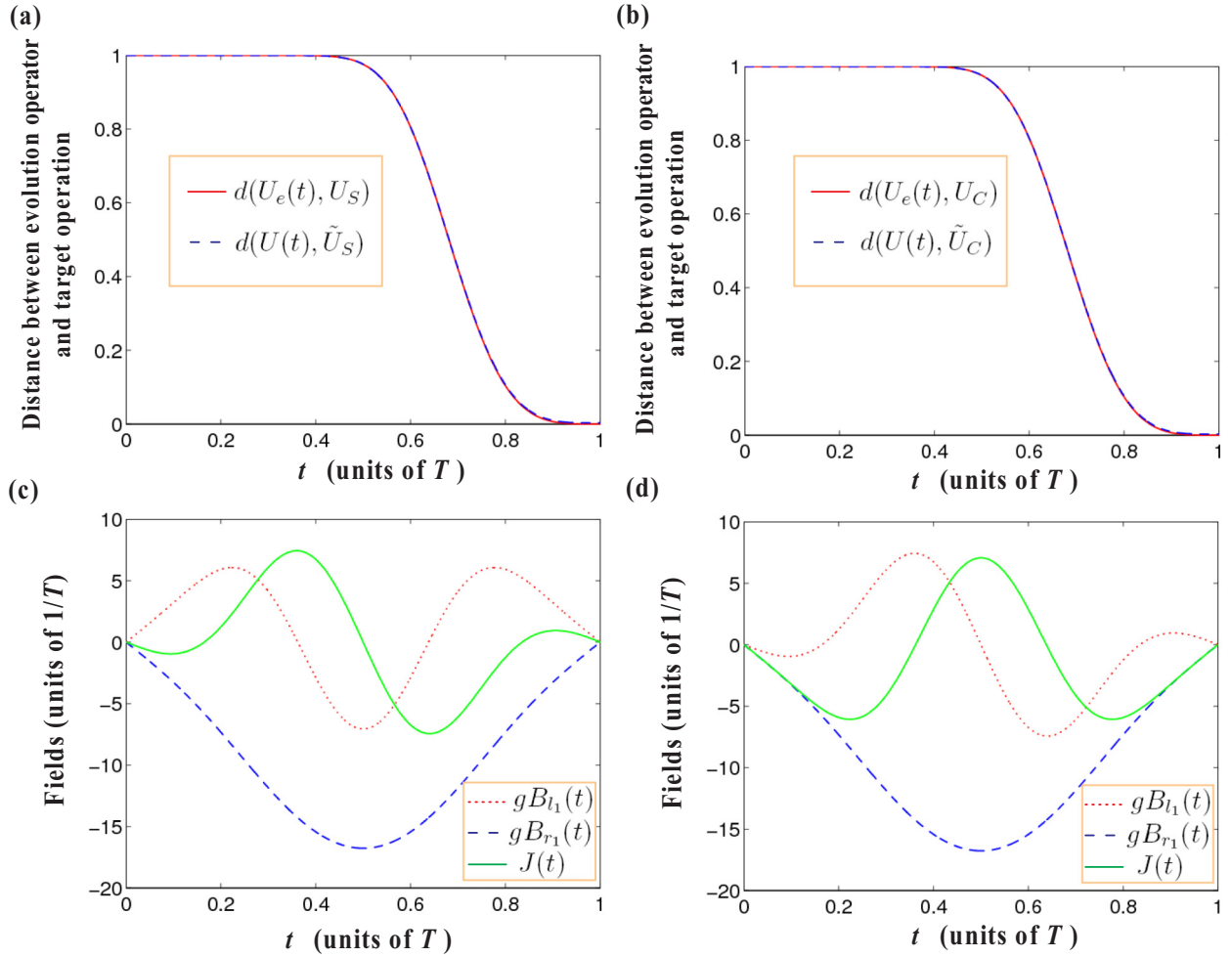


FIG. 1. (a) $d(U_e(t), U_S)$ and $d(U(t), \tilde{U}_S)$ versus t . (b) $d(U_e(t), U_C)$ and $d(U(t), \tilde{U}_C)$ versus t . (c) $gB_{l_1}(t)$, $gB_{r_1}(t)$, and $J(t)$ versus t in the implementations of the S gate. (d) $gB_{l_1}(t)$, $gB_{r_1}(t)$, and $J(t)$ versus t in the implementations of the C gate.

of $R(t)$. In addition, $\Delta_1 = 0$ and $\Delta_2 = 400/T$ are selected for the condition $\Omega_{\max} \ll |2\Delta_1 - \Delta_2|$, and in this case, $\tilde{B}_l(t)$ and $\tilde{B}_r(t)$ are fixed along the y and x axis, respectively. Seen from the blue-dashed lines in the Figs. 1(a) and 1(b), we find that the evolutions governed by the original Hamiltonian $H(t)$ match well with that governed by the effective Hamiltonian $H_e(t)$. Moreover, we obtained the distances as $d(U(T), \tilde{U}_S) = 0.0032$ and $d(U(T), \tilde{U}_C) = 0.0029$. Therefore, the implementations of the S gate and the C gate can be realized with the original Hamiltonian $H(t)$.

V. ANALYSIS OF ERRORS AND NOISE

Since there may exist imperfections in real experiments due to the influences of the errors and noise, the analysis of the robustness against these disturbing factors is helpful for estimating the performance of the scheme in a practical environment. As examples to test the robustness of the scheme, we perform numerical simulations for the implementations of the S gate and the C gate in Sec. IV B.

Because the realization of the geometric gates in the scheme is based on the driving of the control fields, the errors of the control fields may decrease the fidelities of the

implementations of the geometric gates. Therefore, we first focus on the systematic errors of the control fields. For the implementations of the S gate and the C gate, we assume that the erroneous control fields of $B_{l_1}(t)$, $B_{r_1}(t)$, and $J(t)$ are $(1 + \delta_1)B_{l_1}(t)$, $(1 + \delta_2)B_{r_1}(t)$, and $(1 + \delta_3)J(t)$, respectively, where δ_1 , δ_2 , and δ_3 denote the coefficients of the systematic errors of the corresponding control fields. By substituting the erroneous control fields in the numerical simulations, we plot the distances $d(U(T), \tilde{U}_S)$ and $d(U(T), \tilde{U}_C)$ versus δ_n ($n = 1, 2, 3$) in Figs. 2(a) and 2(b), respectively. According to Fig. 2, both the implementations of the S gate and C gate are insensitive to the systematic errors of $B_{l_1}(t)$ and $J(t)$, while are relatively sensitive to the error of $B_{r_1}(t)$. Since the fourth component of the eigenvector $|\tilde{\phi}_1(t)\rangle$ for the dynamic invariant keeps unchanged in the evolution with $\eta(t) = 0$, the variations of the remaining three components can be described by a curve on a sphere of a three-dimensional parameter space by defining the axes as $x_p = \sin \theta \sin \varphi$, $y_p = \sin \theta \cos \varphi$, and $z_p = \cos \theta$. Considering that the trajectories of (x_p, y_p, z_p) can help us to analyze the influence of the systematic errors to the shape of the evolution paths, we plot the trajectories of (x_p, y_p, z_p) with $\delta_n = 0$, $\delta_1 = -0.1$, $\delta_2 = -0.1$, and

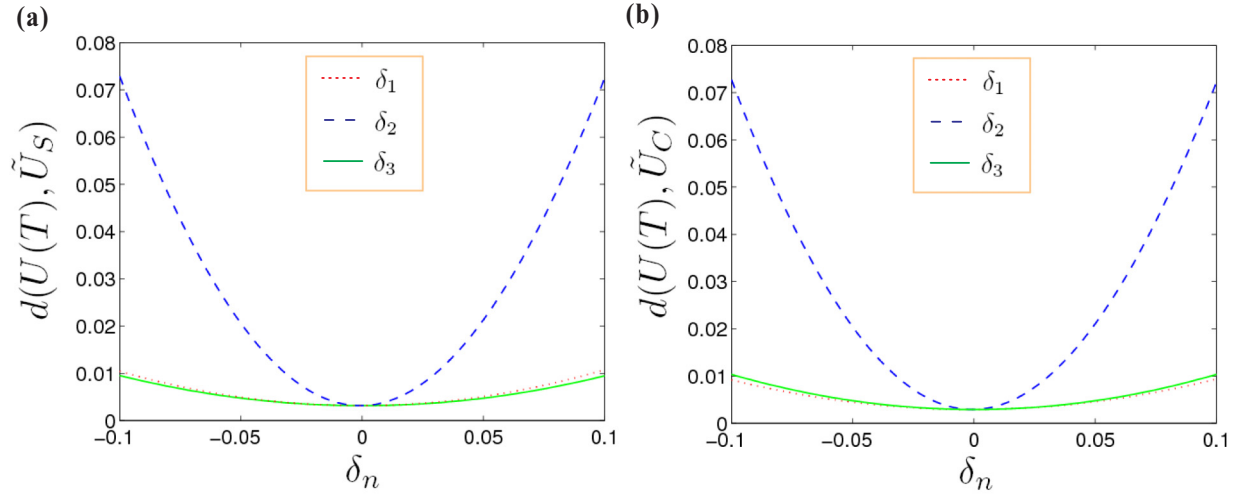


FIG. 2. (a) $d(U(T), \tilde{U}_S)$ versus δ_n ($n = 1, 2, 3$). (b) $d(U(T), \tilde{U}_C)$ versus δ_n .

$\delta_3 = -0.1$ on a sphere in Fig. 3 in the implementations of the C gate ($\varphi_0 = -\pi/2$). The trajectory of (x_p, y_p, z_p) without the systematic errors is shown by the red solid line in Fig. 3, where we can find that the height z_p of the curve is unchanged after the evolution, and the trajectory is approximate to a circle with $\theta = \pi/4, \varphi \in [0, 2\pi)$. Moreover, as shown by the orange dashed line and the blue dotted line in Fig. 3, the trajectories of (x_p, y_p, z_p) under the influences of the systematic errors of control fields $B_{l_1}(t)$ and $J(t)$ are nearly closed loop with very slight changes of height z_p . Furthermore, seen from the magenta dashed-dotted line in Fig. 3, under the influence of the systematic errors of control field $B_{r_1}(t)$, the trajectory of (x_p, y_p, z_p) deviates from a closed loop with the height z_p changed in the evolution. With the trajectories plotted in Fig. 3, the sensitiveness of the scheme to the systematic errors of different control fields can be summed up as follows. On one hand, the geometric phases acquired in the evolution are mainly dependent on the global property of the evolution

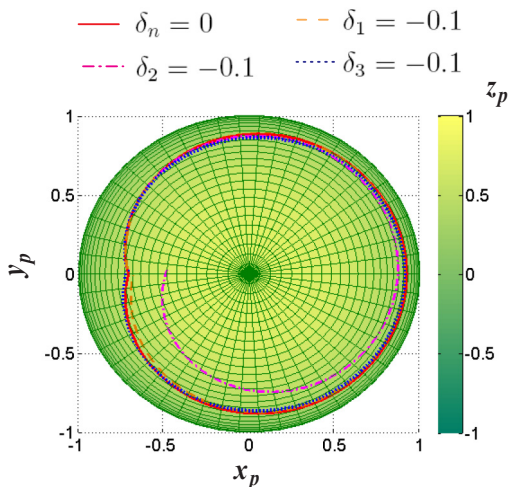


FIG. 3. The trajectories of $(x_p = \sin \theta \sin \varphi, y_p = \sin \theta \cos \varphi, z_p = \cos \theta)$ on a three-dimensional sphere ($\varphi_0 = -\pi/2$) with $\delta_n = 0$ (red solid line), $\delta_1 = -0.1$ (orange dashed line), $\delta_2 = -0.1$ (magenta dashed-dotted line), and $\delta_3 = -0.1$ (blue dotted line).

paths. On the other hand, the shapes of the evolution paths are mainly changed by the systematic error of the field $B_{r_1}(t)$. Thus, the influence of the systematic error of $B_{r_1}(t)$ plays a major role among the systematic errors of all control fields. However, for the fields $B_{l_1}(t)$ and $J(t)$, since they are less related to shape of the evolution paths, the influence of the systematic errors of $B_{l_1}(t)$ and $J(t)$ to the acquired geometric phases is much less than $B_{r_1}(t)$. Even when δ_1 and δ_3 reaches 10%, $d(U(T), \tilde{U}_S)$ and $d(U(T), \tilde{U}_C)$ are only about 0.01, which means the average gate fidelities for S gate and C gate are both higher than 99%. For the systematic errors of $B_{r_1}(t)$, when δ_2 reaches 10%, $d(U(T), \tilde{U}_S)$ and $d(U(T), \tilde{U}_C)$ are about 0.072, i.e., the gate fidelities for S gate and C gate are both still higher than 92.8%. If we can control the systematic errors of $B_{r_1}(t)$ within 5%, the gate fidelities for S gate and C gate can be higher than 98%. Thus, the scheme is robust against the systematic errors of the control fields in a certain degree.

Apart from the systematic errors, the random noise is also a source inducing the imperfect operations in a real experiment. Therefore, studying the implementations of the quantum gates in a noisy environment is also helpful to estimate the performance of the scheme. As the additive white Gaussian noise (AWGN) is a nice model for emulating the effect of many stochastic processes, we investigate the implementations of the S gate and the C gate by adding AWGN to the control fields. The control fields with AWGN read as

$$\begin{aligned} B'_{l_1}(t) &= B_{l_1}(t) + \text{AWGN}(B_{l_1}(t), \zeta), \\ B'_{r_1}(t) &= B_{r_1}(t) + \text{AWGN}(B_{r_1}(t), \zeta), \\ J'(t) &= J(t) + \text{AWGN}(J(t), \zeta), \end{aligned} \quad (52)$$

in which $\text{AWGN}(\cdot, \zeta)$ denote a function to generate AWGN with the signal-to-noise ratio (SNR) ζ for the corresponding control field. Because the AWGN behave randomly in every single simulation, to estimate the effect of AWGN, we should perform repeated simulations for an average. Hence, we respectively perform 10 times of simulations for the implementations of S gate and C gate with SNRs $\zeta = 10$, $\zeta = 5$, and $\zeta = 2$. Distances $d(U(T), \tilde{U}_S)$ and $d(U(T), \tilde{U}_C)$

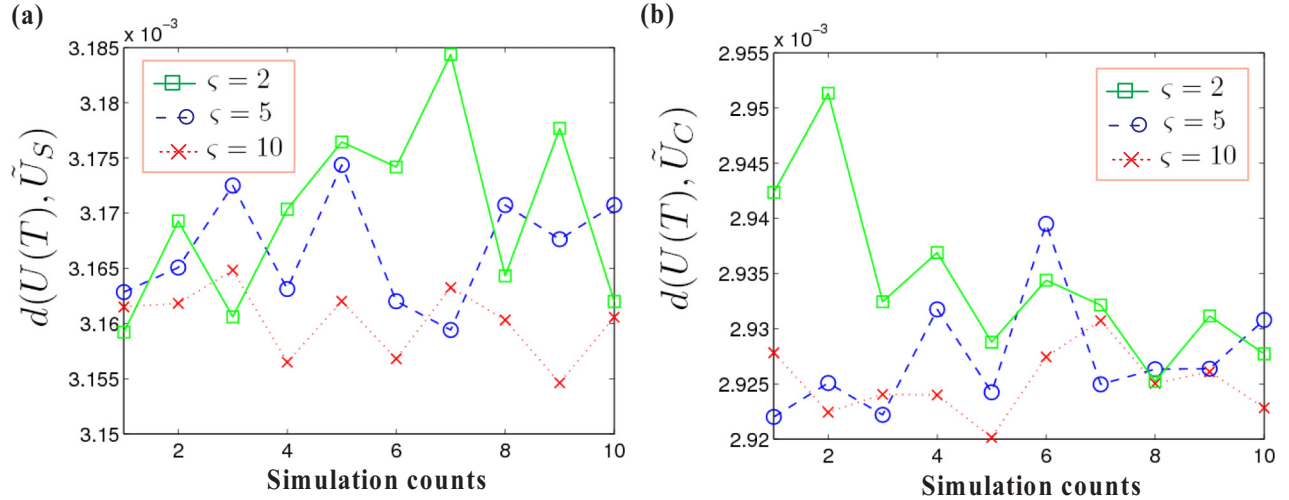


FIG. 4. (a) $d(U(T), \tilde{U}_S)$ in the implementation of the S gate under the influence of AWGN versus simulation counts. (b) $d(U(T), \tilde{U}_C)$ in the implementation of the C gate under the influence of AWGN versus simulation counts.

in each repeated simulation are shown in Figs. 4(a) and 4(b), respectively. According to Fig. 4, when the AWGN is added, the distances $d(U(T), \tilde{U}_S)$ and $d(U(T), \tilde{U}_C)$ are, respectively, fluctuating around 0.0032 and 0.0029 [the values of distances $d(U(T), \tilde{U}_S)$ and $d(U(T), \tilde{U}_C)$ obtained in the case without AWGN]. Moreover, when decreasing the SNR, the fluctuations of $d(U(T), \tilde{U}_S)$ and $d(U(T), \tilde{U}_C)$ become more significant. However, even when $\zeta = 2$, $d(U(T), \tilde{U}_S)$ and $d(U(T), \tilde{U}_C)$ are still approximate to 0.0032 and 0.0029, respectively. Thus, the scheme is robust against AWGN. The robustness of the scheme to the AWGN is not hard to be understood. Since the AWGN produce random values added on the original control fields with zero average, the total effect of AWGN to the shape of the evolution paths are nearly neutralized, i.e., the AWGN only makes the trajectories in the parameter spaces slightly fluctuate around the original ones. As the geometric phases are mainly dependent on the global property of the evolution paths, the local fluctuations do not lead much errors in the accumulations of geometric phases. Accordingly, the advantage of the geometric phase makes the scheme insensitive to the random noise.

Finally, the resonant conditions in Eq. (32) are also key points to successfully realize the scheme. Since Δ_1 and Δ_2 are also controlled by the fields in the scheme, it is also necessary to discuss the influence of the errors of Δ_1 and Δ_2 to the scheme. Here, we consider that the Δ_1 and Δ_2 have perturbations as $\delta\Delta_1$ and $\delta\Delta_2$, respectively. To compare the perturbations of Δ_1 and Δ_2 with other control fields, Ω_{\max} shown in Eq. (51) is used as the unit of the perturbations in the following discussions. We plot the distances $d(U(T), \tilde{U}_S)$ and $d(U(T), \tilde{U}_C)$ versus $\delta\Delta_1$ and $\delta\Delta_2$ in Figs. 5(a) and 5(b), respectively. As shown in Fig. 5, both the implementations of S gate and C gate are insensitive to the perturbations of Δ_2 , while are more sensitive to the perturbations of Δ_1 . This is because in the implementations of S gate and C gate, we set $B_{l_2}(t)$ and $B_{r_2}(t)$ as zeros. Thus, the condition $\omega_{l_2} = \omega_{r_2} = \Delta_1 - \Delta_2$ is not so important, and we just need to ensure that the condition $|gB_{l_1}(t)|, |gB_{r_1}(t)| \ll |\Delta_1 - \Delta_2|$ is fulfilled. However, since the fields $B_{l_1}(t)$ and $B_{r_1}(t)$ are used in

the implementations of S gate and C gate, the condition $\omega_{l_1} = \omega_{r_1} = -\Delta_1$ is still important. When $\delta\Delta_1/\Omega_{\max}$ and $\delta\Delta_2/\Omega_{\max}$ are controlled within 5%, the worst situations for the implementations of S gate and C gate both appear at $\delta\Delta_1/\Omega_{\max} = \delta\Delta_2/\Omega_{\max} = -5\%$, where we obtain $d(U(T), \tilde{U}_S) = 0.0858$ and $d(U(T), \tilde{U}_C) = 0.0946$, respectively. The results show the scheme also possesses some robustness against the perturbations of Δ_1 and Δ_2 .

VI. CONCLUSION

In conclusion, we have proposed a flexible scheme to realize nonadiabatic geometric quantum gates based on the NHQC+ and the IBRE. First, we showed the approach to make the IBRE cooperate with NHQC+. Thus, a compound, the NHQC + IBRE, was built up for multipaths nonadiabatic geometric quantum computation. With the flexibility of the NHQC + IBRE, the scheme showed advantages in many ways. (i) Different types of nonadiabatic geometric quantum gates can be readily constructed with only the adjustment of the boundary conditions of control parameters. (ii) The full uses of the multiple evolution paths are helpful to reduce the requirements of energy levels of quantum systems. Consequently, the NHQC + IBRE can be even realized without any auxiliary levels or qubits. This may simplify the physical implementations of quantum gates in several cases. For example, in the implementation of the geometric two-qubit gate of spin qubits in the scheme, the computational basis $\{|\uparrow\uparrow\rangle, |\uparrow\downarrow\rangle, |\downarrow\uparrow\rangle, |\downarrow\downarrow\rangle\}$ spanned the full space of states of two spins. To implement the HNQC in a standard way, the condition in Eq. (16) implies that the Hamiltonian should be always a null matrix. Therefore, auxiliary spin qubits are required. However, in the current scheme, the implementation of geometric two-qubit gates can be achieved with only two spins. (iii) The dynamic invariant can be constructed with the help of Lie algebra, which provides a powerful tool to study the nonadiabatic geometric quantum computation in various physical systems possessing different dynamic symmetry. To show the applications of the scheme, we considered the implementation of nontrivial two-qubit gates

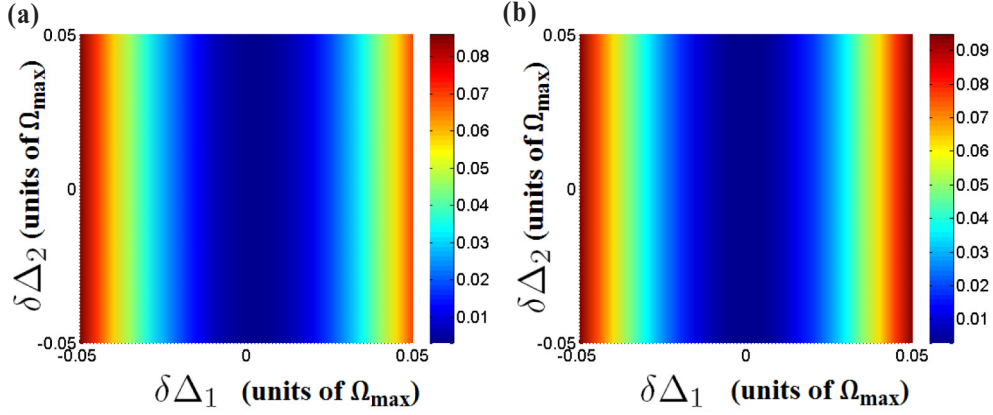


FIG. 5. (a) $d(U(T), \tilde{U}_s)$ versus $\delta\Delta_1$ and $\delta\Delta_2$. (b) $d(U(T), \tilde{U}_c)$ versus $\delta\Delta_1$ and $\delta\Delta_2$.

of spin qubits in a double-quantum-dot system. We also estimated the performance of the quantum gates with the numerical simulations. The results demonstrated that the scheme holds robustness against systematic errors of the control fields, the influence of the random noise, and the perturbations in the resonant conditions. Therefore, the scheme may provide some useful perspectives for the implementations of high-fidelity nonadiabatic geometric quantum gates.

ACKNOWLEDGMENTS

This work was supported by the National Natural Science Foundation of China under Grants No. 11575045, No. 11674060, No. 2018J01414, and No. 11805036.

APPENDIX A: ARBITRARY SINGLE-QUBIT NONADIABATIC GEOMETRIC QUANTUM GATES WITH NHQC + IBRE

We consider that a spin is driven by a magnetic field $\vec{B}(t) = B_x(t)\vec{e}_x + B_y(t)\vec{e}_y + B_z(t)\vec{e}_z$. The Hamiltonian of the system is

$$H_s(t) = g\vec{B}(t) \cdot \vec{S}, \quad (\text{A1})$$

with $\vec{S} = S_x\vec{e}_x + S_y\vec{e}_y + S_z\vec{e}_z$ being the spin operator of the spin. The dynamics of the system can be investigated by the $su(2)$ Lie algebra with generators

$$\sigma_x = \begin{bmatrix} 0 & 1 \\ 1 & 0 \end{bmatrix}, \quad \sigma_y = \begin{bmatrix} 0 & -i \\ i & 0 \end{bmatrix},$$

$$\sigma_z = \begin{bmatrix} 1 & 0 \\ 0 & -1 \end{bmatrix}. \quad (\text{A2})$$

We assume that the dynamic invariant $I_s(t)$ of the single spin is

$$I_s(t) = \xi_x(t)\sigma_x + \xi_y(t)\sigma_y + \xi_z(t)\sigma_z. \quad (\text{A3})$$

With the help of Eq. (14), one can derive

$$\dot{\xi}_x = B_y\xi_z - B_z\xi_y, \quad \dot{\xi}_y = B_z\xi_x - B_x\xi_z, \quad \dot{\xi}_z = B_x\xi_y - B_y\xi_x. \quad (\text{A4})$$

As the rank of matrix

$$\mathcal{M}_s(t) = \frac{1}{2} \begin{bmatrix} 0 & \xi_z & -\xi_y \\ -\xi_z & 0 & \xi_x \\ \xi_y & \xi_x & 0 \end{bmatrix} \quad (\text{A5})$$

is 2, a constraint equation for $\{\xi_x, \xi_y, \xi_z\}$ can be found:

$$\xi_x^2 + \xi_y^2 + \xi_z^2 = \mathcal{C}^2, \quad (\text{A6})$$

with a real constant \mathcal{C} . By parametrizing $\{\xi_x, \xi_y, \xi_z\}$ with $\mathcal{C} = 1$, we have

$$\xi_x = \sin \chi \sin \zeta, \quad \xi_y = \sin \chi \cos \zeta, \quad \xi_z = \cos \chi. \quad (\text{A7})$$

Resolving Eq. (A4) with the parametrizations in Eq. (A7), the control fields are derived as

$$B_x(t) = (B_z + \dot{\zeta}) \sin \zeta \tan \chi - \dot{\chi} \cos \zeta, \quad (\text{A8})$$

$$B_y(t) = (B_z + \dot{\zeta}) \cos \zeta \tan \chi + \dot{\chi} \sin \zeta.$$

The eigenvectors of $I_s(t)$ can be also derived with Eq. (A7) as

$$|\phi_1^s(t)\rangle = \begin{bmatrix} \cos \frac{\chi}{2} \\ ie^{-i\zeta} \sin \frac{\chi}{2} \end{bmatrix}, \quad |\phi_2^s(t)\rangle = \begin{bmatrix} ie^{i\zeta} \sin \frac{\chi}{2} \\ \cos \frac{\chi}{2} \end{bmatrix}. \quad (\text{A9})$$

The time derivatives of the dynamic phases $\vartheta_1^s(t)$, $\vartheta_2^s(t)$ and the geometric phases $\Theta_1^s(t)$, $\Theta_2^s(t)$ acquired by $|\phi_1^s(t)\rangle$ and $|\phi_2^s(t)\rangle$, respectively, read as

$$\dot{\vartheta}_1^s(t) = -\frac{1}{2} \sec \chi (B_z + \dot{\zeta} \sin^2 \chi), \quad \dot{\vartheta}_2^s(t) = -\dot{\vartheta}_1^s(t),$$

$$\dot{\Theta}_1^s(t) = \dot{\zeta} \sin^2 \frac{\chi}{2}, \quad \dot{\Theta}_2^s(t) = -\dot{\Theta}_1^s(t). \quad (\text{A10})$$

Therefore, to eliminate the dynamic phases, $B_z(t) = -\dot{\zeta} \sin^2 \chi$ is a choice. Thus, the evolution of the single spin after a cycling evolution becomes

$$U_s(T) = \begin{bmatrix} \cos \Theta_s + i \cos \chi \sin \Theta_s & e^{i\zeta} \sin \chi \sin \Theta_s \\ -e^{-i\zeta} \sin \chi \sin \Theta_s & \cos \Theta_s - i \cos \chi \sin \Theta_s \end{bmatrix}$$

$$= e^{i\Theta_s \vec{n} \cdot \vec{\sigma}}, \quad (\text{A11})$$

where we have

$$\Theta_s = \int_0^T \dot{\zeta}(t) \sin^2 \left[\frac{\chi(t)}{2} \right] dt, \quad \vec{n} = \xi_x \vec{e}_x + \xi_y \vec{e}_y + \xi_z \vec{e}_z,$$

$$\vec{\sigma} = \sigma_x \vec{e}_x + \sigma_y \vec{e}_y + \sigma_z \vec{e}_z. \quad (\text{A12})$$

$U_s(T)$ shown in Eq. (A11) represents a rotation which can generate a set of universal single-qubit gates [48]. As an example, we discuss the design of parameters for the realization

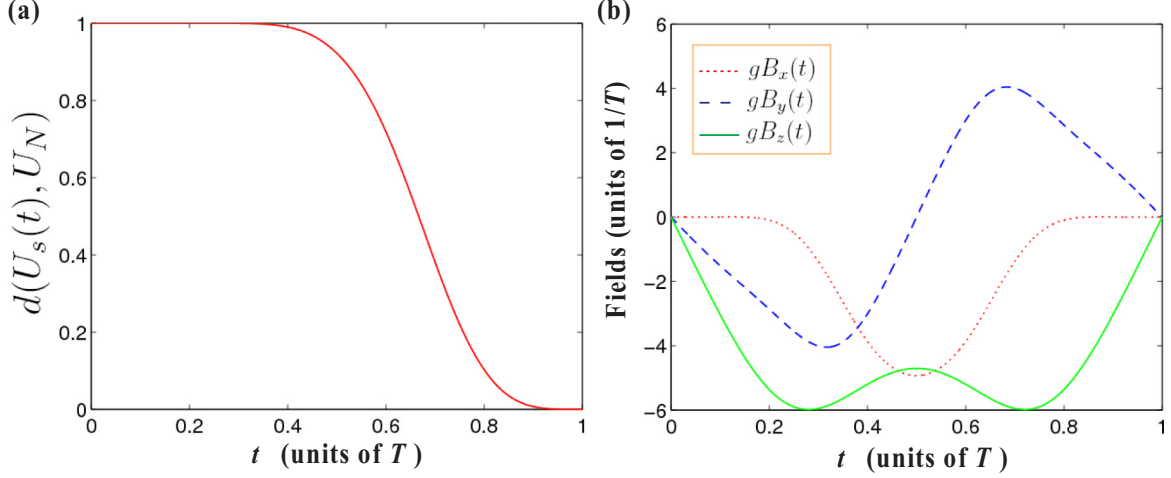


FIG. 6. (a) $d(U_s(t), U_N)$ versus t . (b) $gB_x(t)$, $gB_y(t)$, and $gB_z(t)$ versus t .

of the NOT gate U_N [$\zeta(0) = \pi/2$, $\chi(0) = \pi/2$, $\Theta_s = \pi/2$]. For a cycling evolution, the parameters are selected as

$$\begin{aligned}\zeta(t) &= \frac{\pi}{2} + \pi \left[1 - \cos\left(\frac{\pi t}{T}\right) \right], \\ \chi(t) &= \frac{\pi}{2} - \Upsilon_s \sin^2\left(\frac{\pi t}{T}\right),\end{aligned}\quad (\text{A13})$$

with Υ_s being a time-independent parameter. To obtain $\Theta_s = \pi/2$, we obtain $\Upsilon_s = 0.8089$ by numerically calculating Eq. (A12). We plot the distance $d(U_s(t), U_N)$ versus t/T in Fig. 6(a). Moreover, $gB_x(t)$, $gB_y(t)$, and $gB_z(t)$ versus t/T are plotted in Fig. 6(b). Seen from Fig. 6, the NOT gate can be successfully implemented with NHQC + IBRE.

APPENDIX B: EXISTENCE OF THE OPERATOR $\tilde{\Xi}_\ell(t)$ SATISFYING THE VON NEUMANN EQUATION FOR DEGENERATE EIGENVECTORS OF THE INVARIANT

Assuming \mathcal{E} is the set of all the eigenvectors of $I(t)$, \mathcal{E}_1 is a subset of \mathcal{E} containing all the degenerate eigenvectors of $I(t)$, and \mathcal{D} is the set of all the solutions of the Schrödinger equation. On one hand, according to the Lewis-Riesenfeld invariant theory, for a nondegenerate eigenvector $|\phi_\ell(t)\rangle \in \mathcal{E} - \mathcal{E}_1$ of $I(t)$, $|\psi_\ell(t)\rangle = e^{i\alpha_\ell(t)}|\phi_\ell(t)\rangle$ [$\alpha_\ell(t)$ is the Lewis-Riesenfeld phase of $|\phi_\ell(t)\rangle$] is a solution of the Schrödinger equation. Therefore, one can build a subset of \mathcal{D} as

$$\mathcal{D}_2 = \{|\psi_\ell(t)\rangle = e^{i\alpha_\ell(t)}|\phi_\ell(t)\rangle | |\phi_\ell(t)\rangle \in \mathcal{E} - \mathcal{E}_1\}. \quad (\text{B1})$$

On the other hand, based on the completeness of \mathcal{E} and \mathcal{D} , the degenerate eigenvectors $|\phi_\ell(t)\rangle \in \mathcal{E}_1$ can be expressed by the superpositions of solutions in $\mathcal{D}_1 = \mathcal{D} - \mathcal{D}_2$ as $|\phi_\ell(t)\rangle = V_1(t)|\psi_\ell(t)\rangle$ via a unitary operator $V_1(t)$ [$|\psi_\ell(t)\rangle \in \mathcal{D}_1$, $V_1(t)|\psi_\ell(t)\rangle \in \mathcal{E}_1$]. Thus, one can obtain $|\psi_\ell(t)\rangle = V_1^\dagger(t)|\phi_\ell(t)\rangle$ on the contrary. Consequently, $|\psi_\ell(t)\rangle$ is also an eigenvector of $I(t)$ as it can be expanded by degenerate eigenvectors $|\phi_\ell(t)\rangle \in \mathcal{E}_1$. Since the density operator $\rho_\ell(t) = |\psi_\ell(t)\rangle\langle\psi_\ell(t)|$ satisfies the von Neumann equation $\frac{d}{dt}\tilde{\rho}_\ell(t) = -i[H(t), \tilde{\rho}_\ell(t)]$, $V_1^\dagger(t)$ provide a way of superposition to construct redefined operator $\tilde{\Xi}'_\ell(t)$. Noticing that for an arbitrary

angle $\zeta(t)$, $e^{i\zeta(t)}|\psi_\ell(t)\rangle$ can also be used in constructing $\tilde{\Xi}'_\ell(t)$ to satisfy the von Neumann equation, $V_1^\dagger(t)$ is not the only choice of the superpositions. Thus, we have the conclusions that there exist multiple choices for the coefficients of the superpositions to find $\tilde{\Xi}'_\ell(t)$ obeying the von Neumann equation. When substituting the redefined degenerate eigenvectors $\{|\tilde{\phi}_\ell(t)\rangle\} \in \text{span}\{\mathcal{E}_1\}$ into the von Neumann equation, we can derive the condition to make the von Neumann equation satisfied is

$$\langle\tilde{\phi}_\ell(t)| \left[i\frac{\partial}{\partial t} - H(t) \right] |\tilde{\phi}_{\ell'}(t)\rangle = 0 \quad (\ell \neq \ell'). \quad (\text{B2})$$

Therefore, for an \tilde{N} -fold degenerate eigenvalue, the number of independent conditions to construct redefined operator $\tilde{\Xi}'_\ell(t)$ is $\tilde{N}(\tilde{N} - 1)/2$.

As an example to construct the superposition, we show how to derive the coefficients $\beta_1(t)$ and $\beta_2(t)$ of superpositions in a twofold-degenerate subspace with Eq. (26). By substituting Eq. (26) into the equation

$$\langle\tilde{\phi}_{\ell_2}(t)| \left[i\frac{\partial}{\partial t} - H(t) \right] |\tilde{\phi}_{\ell_1}(t)\rangle = 0, \quad (\text{B3})$$

we derive

$$\begin{aligned}\sin 2\beta_1[\gamma_{11}(t) + \gamma_{22}(t) + i\dot{\beta}_2(t)]/2 - \cos^2 \beta_1 e^{-i\beta_2} \gamma_{12}^*(t) \\ + \sin^2 \beta_1 e^{i\beta_2} \gamma_{12}(t) - \dot{\beta}_1(t) = 0,\end{aligned}\quad (\text{B4})$$

with

$$\gamma_{qq'}(t) = \langle\phi_{\ell_q}(t)| \left[i\frac{\partial}{\partial t} - H(t) \right] |\phi_{\ell_{q'}}(t)\rangle \quad (q, q' = 1, 2). \quad (\text{B5})$$

If $\gamma_{qq}(t) \neq 0$, we first construct two new vectors $|\bar{\phi}_1(t)\rangle = e^{i\Gamma_{11}(t)}|\phi_1(t)\rangle$ and $|\bar{\phi}_2(t)\rangle = e^{i\Gamma_{22}(t)}|\phi_2(t)\rangle$ with $\Gamma_{qq}(t) = \int_0^t \gamma_{qq}(t')dt'$. In this case, we have

$$\bar{\gamma}_{qq}(t) = \langle\bar{\phi}_{\ell_q}(t)| \left[i\frac{\partial}{\partial t} - H(t) \right] |\bar{\phi}_{\ell_q}(t)\rangle = 0. \quad (\text{B6})$$

Therefore, the condition for $\beta_1(t)$ and $\beta_2(t)$ can be simplified as

$$i\dot{\beta}_2(t) \sin 2\beta_1/2 - \cos^2 \beta_1 e^{-i\beta_2} \dot{\gamma}_{12}^*(t) + \sin^2 \beta_1 e^{i\beta_2} \dot{\gamma}_{12}(t) - \dot{\beta}_1(t) = 0, \quad (\text{B7})$$

with

$$\dot{\gamma}_{12}(t) = \langle \bar{\phi}_{\ell_1}(t) | \left[i \frac{\partial}{\partial t} - H(t) \right] | \bar{\phi}_{\ell_2}(t) \rangle. \quad (\text{B8})$$

Assuming $|\dot{\gamma}_{12}(t)| = \bar{\gamma}(t)$ and $\arg[\dot{\gamma}_{12}(t)] = \nu(t)$, we have

$$\begin{aligned} \dot{\beta}_1 &= -\bar{\gamma} \cos 2\beta_1 \cos(\beta_2 + \nu), \\ \dot{\beta}_2 &= -2\bar{\gamma} \csc 2\beta_1 \sin(\beta_2 + \nu). \end{aligned} \quad (\text{B9})$$

With the equation above, it is possible to obtain numerical solutions for $\beta_1(t)$ and $\beta_2(t)$. The solution becomes very simple when $\nu = 0$, where we can obtain time independent β_1 and β_2 as $\beta_1 = \pi/4$ and $\beta_2 = 0$, respectively.

APPENDIX C: RELATION BETWEEN LIE ALGEBRAS $\mathfrak{so}(4)$ AND $\mathfrak{so}(4)$

We now show that the Lie algebra $\mathfrak{so}(4)$ is isomorphic to the Lie algebra $\mathfrak{so}(4)$, and thus the Lie algebra $\mathfrak{so}(4)$ can inherit the properties of $\mathfrak{so}(4)$ up to isomorphism. First, the generators of Lie algebra $\mathfrak{so}(4)$ can be derived via the rotation matrices in group $\text{SO}(4)$,

$$R_{\varrho, \varrho'}(\varpi_{\varrho, \varrho'}) = \mathbb{1} + [\cos(\varpi_{\varrho, \varrho'}) - 1](|\varrho\rangle\langle\varrho| + |\varrho'\rangle\langle\varrho'|) + \sin(\varpi_{\varrho, \varrho'}) (|\varrho'\rangle\langle\varrho| - |\varrho\rangle\langle\varrho'|), \quad (\text{C1})$$

with $\varrho, \varrho' \in \{1, 2, 3, 4\}$, $\varrho < \varrho'$ and $\mathbb{1}$ being the identity operator, as

$$\tilde{G}_{\varrho, \varrho'} = i \frac{\partial}{\partial \varpi_{\varrho, \varrho'}} R_{\varrho, \varrho'}(\varpi_{\varrho, \varrho'})|_{\varpi_{\varrho, \varrho'}=0} = i(|\varrho'\rangle\langle\varrho| - |\varrho\rangle\langle\varrho'|), \quad (\text{C2})$$

which is an antisymmetric matrix with pure imaginary elements. Then, we construct a mapping $\mathcal{F} : \mathfrak{so}(4) \mapsto \mathfrak{so}(4)$ as

$$\begin{aligned} \mathcal{F}(\tilde{G}_{12}) &= G_1, & \mathcal{F}(\tilde{G}_{13}) &= G_5, & \mathcal{F}(\tilde{G}_{14}) &= G_4, \\ \mathcal{F}(\tilde{G}_{23}) &= G_3, & \mathcal{F}(\tilde{G}_{24}) &= G_6, & \mathcal{F}(\tilde{G}_{34}) &= G_2. \end{aligned} \quad (\text{C3})$$

In fact, the mapping \mathcal{F} is a one-to-one mapping, and it can be considered as a representation transform with a unitary operator

$$\tilde{V} = i(|1\rangle\langle 1| + |3\rangle\langle 3|) + (|2\rangle\langle 2| + |4\rangle\langle 4|). \quad (\text{C4})$$

Therefore, we have

$$\begin{aligned} [G_1, G_2] &= [\mathcal{F}(\tilde{G}_{12}), \mathcal{F}(\tilde{G}_{34})] \\ &= [\tilde{V}^\dagger \tilde{G}_{12} \tilde{V}, \tilde{V}^\dagger \tilde{G}_{34} \tilde{V}] = [\tilde{G}_{12}, \tilde{G}_{34}]. \end{aligned} \quad (\text{C5})$$

Similarly, one can obtain the results that for any pair of generators in $\mathfrak{so}(4)$ and the corresponding pairs of generators in $\mathfrak{so}(4)$, the commutation operations are preserved by the mapping \mathcal{F} . Consequently, \mathcal{F} is an isomorphic mapping between $\mathfrak{so}(4)$ and $\mathfrak{so}(4)$, and we can say $\mathfrak{so}(4)$ and $\mathfrak{so}(4)$ are isomorphic.

APPENDIX D: RANK OF MATRIX $\mathcal{M}(t)$ WITH $\mathfrak{so}(N)$ LIE ALGEBRA

Let us show that the rank of matrix $\mathcal{M}(t)$ is always less than the numbers of generators when the Hamiltonian and the invariant are described with $\mathfrak{so}(N)$ ($N \geq 3$) Lie algebras. First, for any generator of Lie algebra $\mathfrak{so}(N)$, we define an operation $\mathcal{L}_{\varrho, \varrho'}$ acting on an arbitrary element X of $\mathfrak{so}(N)$ as

$$\mathcal{L}_{\varrho, \varrho'} X = -i[\tilde{G}_{\varrho, \varrho'}, X], \quad (\text{D1})$$

which can be written as a matrix in basis $\{\tilde{G}_{\varrho, \varrho'} | \varrho, \varrho' = 1, 2, \dots, N, \varrho < \varrho'\}$. Considering the fact that $[\tilde{G}_{\varrho, \varrho'}, \tilde{G}_{\tilde{\varrho}, \tilde{\varrho}'}] = 0$ happens in two cases: (i) $\varrho = \tilde{\varrho}$ and $\varrho' = \tilde{\varrho}'$; (ii) any two indexes of $\varrho, \varrho', \tilde{\varrho}$, and $\tilde{\varrho}'$ are different with each other, the rank of $\mathcal{L}_{\varrho, \varrho'}$ is always less than the total number $[N(N-1)/2]$ of generators of $\mathfrak{so}(N)$. For example, for $\mathfrak{so}(4)$ Lie algebra, we have $[\tilde{G}_{12}, \tilde{G}_{12}] = 0$ and $[\tilde{G}_{12}, \tilde{G}_{34}] = 0$, thus $\text{rank}[\mathcal{L}_{12}] = 4 < 6$. Besides, as $\varrho, \varrho', \tilde{\varrho}$, and $\tilde{\varrho}'$ are arbitrary indexes in the discussions above, it is not hard to derive

$$\begin{aligned} \text{rank}[\mathcal{L}_{\varrho, \varrho'}] &= \text{rank}[\mathcal{L}_{\tilde{\varrho}, \tilde{\varrho}'}] = [N(N-1) \\ &\quad - (N-2)(N-3)]/2 + 1 = 2(N-2). \end{aligned} \quad (\text{D2})$$

On the other hand, considering two arbitrary elements X and Y in $\mathfrak{so}(N)$, we have the Hilbert-Schmidt inner product

$$\begin{aligned} (X, \mathcal{L}_{\varrho, \varrho'} Y) &= -i \text{Tr}\{X[\tilde{G}_{\varrho, \varrho'}, Y]\} \\ &= i \text{Tr}\{Y[\tilde{G}_{\varrho, \varrho'}, X]\} = -(Y, \mathcal{L}_{\varrho, \varrho'} X), \end{aligned} \quad (\text{D3})$$

$\mathcal{L}_{\varrho, \varrho'}$ is always an antisymmetric matrix in basis $\{\tilde{G}_{\varrho, \varrho'} | \varrho, \varrho' = 1, 2, \dots, N, \varrho < \varrho'\}$. Since $\mathcal{L}_{\varrho, \varrho'}$ and $\mathcal{L}_{\tilde{\varrho}, \tilde{\varrho}'}$ are two antisymmetric matrices with the same rank, there exists a nonsingular matrix $\mathcal{V}_{\tilde{\varrho}, \tilde{\varrho}', \varrho, \varrho'}$ satisfying

$$\mathcal{L}_{\varrho, \varrho'} = \mathcal{V}_{\tilde{\varrho}, \tilde{\varrho}', \varrho, \varrho'}^T \mathcal{L}_{\tilde{\varrho}, \tilde{\varrho}'} \mathcal{V}_{\tilde{\varrho}, \tilde{\varrho}', \varrho, \varrho'}. \quad (\text{D4})$$

Especially when $\tilde{\varrho} = 1$ and $\tilde{\varrho}' = 2$, we have

$$\mathcal{L}_{\varrho, \varrho'} = \tilde{\mathcal{V}}_{\varrho, \varrho'}^T \mathcal{L}_{12} \tilde{\mathcal{V}}_{\varrho, \varrho'}, \quad (\text{D5})$$

with $\tilde{\mathcal{V}}_{\varrho, \varrho'} = \mathcal{V}_{1,2,\varrho,\varrho'}$.

Assuming that the Hamiltonian and the invariant of the system are

$$H(t) = \sum_{\varrho < \varrho'} \tilde{\lambda}_{\varrho, \varrho'}(t) \tilde{G}_{\varrho, \varrho'} \quad (\text{D6})$$

and

$$I(t) = \sum_{\varrho < \varrho'} \tilde{\xi}_{\varrho, \varrho'}(t) \tilde{G}_{\varrho, \varrho'}, \quad (\text{D7})$$

respectively, the matrix $\mathcal{M}(t)$ can be decomposed as

$$\mathcal{M}(t) = \sum_{\varrho < \varrho'} \tilde{\xi}_{\varrho, \varrho'}(t) \mathcal{L}_{\varrho, \varrho'}. \quad (\text{D8})$$

Using the results of Eqs. (D2) and (D5), we can derive

$$\mathcal{M}(t) = \left[\sum_{\varrho < \varrho'} \tilde{\xi}_{\varrho, \varrho'}(t) \tilde{\mathcal{V}}_{\varrho, \varrho'} \right] \mathcal{L}_{12}, \quad (\text{D9})$$

consequently,

$$\begin{aligned} \text{rank}[\mathcal{M}(t)] &\leq \min \left\{ \text{rank} \left[\sum_{\wp < \wp'} \tilde{\lambda}_{\wp, \wp'}(t) \tilde{\mathcal{V}}_{\wp, \wp'} \right], \text{rank}(\mathcal{L}_{12}) \right\} \\ &\leq \text{rank}(\mathcal{L}_{12}) = 2(N-2). \end{aligned} \quad (\text{D10})$$

The results can also be applied to the Lie algebras isomorphic to $\text{so}(N)$. For example, in the implementation of the two-qubit gate in Sec. IV, $\mathfrak{so}(4)$ is isomorphic to $\text{so}(4)$, thus $\text{rank}[\mathcal{M}(t)] \leq 2 \times (4-2) = 4$. Moreover, for the implementation of the single-qubit gate, as $\text{su}(2)$ is isomorphic to $\text{so}(3)$, the rank of $\mathcal{M}_s(t)$ is less or equal to $2 \times (3-2) = 2$. This result indicates that, if a system possesses $\text{so}(N)$ dynamical structure, and the number of available couplings are more than $2(N-2)$, there may exist auxiliary couplings that help us to eliminate the dynamic phases like $J(t)$ in Eq. (49) and $B_z(t)$ below Eq. (A10).

As a side note, we also make some brief discussions about the general Lie algebra to characterize the evolution of an N -dimensional system, namely, the $\text{su}(N)$ algebra. When the dynamical invariant is described by $\text{su}(N)$ algebra, although the rank of matrix $\mathcal{M}(t)$ is more difficult to be estimated, $\mathcal{M}(t)$ can also not be a full-rank matrix as $\mathcal{M}(t)I(t) = -i[I(t), I(t)] = 0$. Since the total number of generators of a $\text{su}(N)$ algebra is $N^2 - 1$, the rank of $\mathcal{M}(t)$ must less or equal to $N^2 - 2$. Interestingly, as

$$\begin{aligned} (X, \mathcal{M}(t)Y) &= -i \text{Tr}\{X[I(t), Y]\} \\ &= i \text{Tr}\{Y[I(t), X]\} = -(Y, \mathcal{M}(t)X), \end{aligned} \quad (\text{D11})$$

$\mathcal{M}(t)$ is always an antisymmetric matrix in the basis of generators, and thus it has even-number rank. When N is odd, the rank of $\mathcal{M}(t)$ must less than $N^2 - 3$. Therefore, for a system holding $\text{su}(N)$ dynamical structure, it may also be possible to find out some couplings in eliminating the dynamic phases.

APPENDIX E: NOTE ABOUT THE SOLUTIONS OF EQ. (14)

First, we consider the case that all the couplings in the considered Lie algebra are available (all elements of $\vec{\lambda}$ can be freely designed). The condition to make the solution exist is

$$\text{rank}(\mathcal{M}(t)) = \text{rank}(\vec{\mathcal{M}}(t)), \quad (\text{E1})$$

with $\vec{\mathcal{M}}(t) = [\mathcal{M}(t)|\dot{\xi}(t)]$ being the augmented matrix for Eq. (14). Assuming that the total number of generators is \mathbb{N} , and the rank of $\mathcal{M}(t)$ is \mathbb{N}_1 , $\vec{\mathcal{M}}(t)$ can be changed into

$$\vec{\mathcal{M}}(t) = \begin{bmatrix} \mathcal{M}'_{\mathbb{N}_1 \times \mathbb{N}}(t) & \mathbb{f}_1(\dot{\xi}) \\ \mathcal{O}_{\mathbb{N}_2 \times \mathbb{N}} & \mathbb{f}_2(\dot{\xi}) \end{bmatrix}, \quad (\text{E2})$$

by a serial of elementary row transformation, where $\mathcal{M}'_{\mathbb{N}_1 \times \mathbb{N}}(t)$ is a rank- \mathbb{N}_1 matrix, $\mathcal{O}_{\mathbb{N}_2 \times \mathbb{N}}$ is a $(\mathbb{N}_2 \times \mathbb{N})$ -dimensional null matrix ($\mathbb{N}_2 = \mathbb{N} - \mathbb{N}_1$), $\mathbb{f}_1(\dot{\xi})$ [$\mathbb{f}_2(\dot{\xi})$] is an \mathbb{N}_1 -dimensional (\mathbb{N}_2 -dimensional) column vector, whose elements are linear superpositions of the elements of $\dot{\xi}$.

Therefore, we obtain the condition to make $\text{rank}(\mathcal{M}(t)) = \text{rank}(\vec{\mathcal{M}}(t))$ satisfied as $\mathbb{f}_2(\dot{\xi}) = 0$. $\mathbb{f}_2(\dot{\xi}) = 0$ is the origin of the constraint equations for $\{\xi_j(t)\}$. Thus, when all the couplings in the considered Lie algebra are available, Eq. (14) can always be solved by adding constraint equations. Similar results have also been shown by previous scheme [67] with Gauss elimination and pseudoinverse matrix. On the other hand, if the Hamiltonian does not contain all the couplings in the considered Lie algebra [some elements of $\vec{\lambda}(t)$ should be zeros], we can divide $\vec{\lambda}$ into two parts and obtain the equation

$$\begin{bmatrix} \mathcal{M}_{\mathbb{N}_1 \times \mathbb{N}_1}^{(1)}(t) & \mathcal{M}_{\mathbb{N}_1 \times \mathbb{N}_2}^{(2)}(t) \\ \mathcal{M}_{\mathbb{N}_2 \times \mathbb{N}_1}^{(3)}(t) & \mathcal{M}_{\mathbb{N}_2 \times \mathbb{N}_2}^{(4)}(t) \end{bmatrix} \begin{bmatrix} \lambda_{\mathbb{N}_1}(t) \\ \mathbb{0}_{\mathbb{N}_2} \end{bmatrix} = \begin{bmatrix} \dot{\xi}_{\mathbb{N}_1}(t) \\ \dot{\xi}_{\mathbb{N}_2}(t) \end{bmatrix}, \quad (\text{E3})$$

where \mathbb{N}_1 is the number of nonzero elements of $\vec{\lambda}$, $\mathbb{N}_2 = \mathbb{N} - \mathbb{N}_1$, $\lambda_{\mathbb{N}_1}(t)$ is the part of $\vec{\lambda}(t)$ with nonzero elements, and $\mathbb{0}_{\mathbb{N}_2}$ is the part of $\vec{\lambda}$ with zero elements. Besides, $\dot{\xi}(t)$ is also divided into two corresponding parts $\dot{\xi}_{\mathbb{N}_1}(t)$ and $\dot{\xi}_{\mathbb{N}_2}(t)$, while the matrix $\mathcal{M}(t)$ is divided into four corresponding blocks as $\mathcal{M}_{\mathbb{N}_1 \times \mathbb{N}_1}^{(1)}(t)$, $\mathcal{M}_{\mathbb{N}_1 \times \mathbb{N}_2}^{(2)}(t)$, $\mathcal{M}_{\mathbb{N}_2 \times \mathbb{N}_1}^{(3)}(t)$, and $\mathcal{M}_{\mathbb{N}_2 \times \mathbb{N}_2}^{(4)}(t)$. Thus, the equation for the reverse engineering reduces to

$$\begin{bmatrix} \mathcal{M}_{\mathbb{N}_1 \times \mathbb{N}_1}^{(1)}(t) \lambda_{\mathbb{N}_1}(t) \\ \mathcal{M}_{\mathbb{N}_2 \times \mathbb{N}_1}^{(3)}(t) \lambda_{\mathbb{N}_1}(t) \end{bmatrix} = \begin{bmatrix} \dot{\xi}_{\mathbb{N}_1}(t) \\ \dot{\xi}_{\mathbb{N}_2}(t) \end{bmatrix}. \quad (\text{E4})$$

Assuming

$$\text{rank} \left(\begin{bmatrix} \mathcal{M}_{\mathbb{N}_1 \times \mathbb{N}_1}^{(1)}(t) \\ \mathcal{M}_{\mathbb{N}_2 \times \mathbb{N}_1}^{(3)}(t) \end{bmatrix} \right) = \mathbb{N}'_1, \quad (\text{E5})$$

we have $\mathbb{N}'_1 = \min\{\mathbb{N}_1, \mathbb{N}_1\}$, and the condition to make the solution of $\lambda_{\mathbb{N}_1}(t)$ exist is

$$\text{rank}[\vec{\mathcal{M}}'(t)] = \text{rank} \left(\begin{bmatrix} \mathcal{M}_{\mathbb{N}_1 \times \mathbb{N}_1}^{(1)}(t) & \dot{\xi}_{\mathbb{N}_1}(t) \\ \mathcal{M}_{\mathbb{N}_2 \times \mathbb{N}_1}^{(3)}(t) & \dot{\xi}_{\mathbb{N}_2}(t) \end{bmatrix} \right) = \mathbb{N}'_1. \quad (\text{E6})$$

By using a serial of elementary row transformation, $\vec{\mathcal{M}}'$ can be changed into

$$\begin{bmatrix} \vec{\mathcal{M}}'_{\mathbb{N}'_1 \times \mathbb{N}_1}(t) & \tilde{\mathbb{f}}_1(\dot{\xi}) \\ \mathcal{O}_{\mathbb{N}'_2 \times \mathbb{N}_1}(t) & \tilde{\mathbb{f}}_2(\dot{\xi}) \end{bmatrix}, \quad (\text{E7})$$

with $\vec{\mathcal{M}}'_{\mathbb{N}'_1 \times \mathbb{N}_1}(t)$ being a rank- \mathbb{N}'_1 matrix, $\mathcal{O}_{\mathbb{N}'_2 \times \mathbb{N}_1}$ being a $(\mathbb{N}'_2 \times \mathbb{N}_1)$ -dimensional null matrix ($\mathbb{N}'_2 = \mathbb{N} - \mathbb{N}'_1$), $\tilde{\mathbb{f}}_1(\dot{\xi})$ [$\tilde{\mathbb{f}}_2(\dot{\xi})$] being an \mathbb{N}'_1 -dimensional (\mathbb{N}'_2 -dimensional) column vector, whose elements are linear superpositions of the elements of $\dot{\xi}$. In this case, the solution of $\lambda_{\mathbb{N}_1}(t)$ exists only if $\tilde{\mathbb{f}}_2(\dot{\xi}) = 0$. $\tilde{\mathbb{f}}_2(\dot{\xi}) = 0$ also produces the constraint equations for $\{\xi_j(t)\}$. Thus, the solution of Eq. (14) always exists by adding proper constraint equations for $\{\xi_j(t)\}$.

- [1] P. W. Shor, in *1994 Proceedings of 35th Annual Symposium on Foundations of Computer Science* (IEEE, Washington DC, 1994).
- [2] L. K. Grover, *Phys. Rev. Lett.* **79**, 325 (1997).
- [3] G. L. Long, *Phys. Rev. A* **64**, 022307 (2001).
- [4] H. F. Hofmann, *Phys. Rev. A* **72**, 022329 (2005).
- [5] B. Paredes, F. Verstraete, and J. I. Cirac, *Phys. Rev. Lett.* **95**, 140501 (2005).
- [6] D. P. O’Leary, G. K. Brennen, and S. S. Bullock, *Phys. Rev. A* **74**, 032334 (2006).
- [7] T. Li and F. G. Deng, *Phys. Rev. A* **94**, 062310 (2016).
- [8] C. P. Yang, Y. X. Liu, and F. Nori, *Phys. Rev. A* **81**, 062323 (2010).
- [9] Y. Li, *Phys. Rev. A* **91**, 052328 (2015).
- [10] A. M. Childs, E. Farhi, and J. Preskill, *Phys. Rev. A* **65**, 012322 (2001).
- [11] L. M. Duan, J. I. Cirac, and P. Zoller, *Science* **292**, 1695 (2001).
- [12] S. L. Zhu and Z. D. Wang, *Phys. Rev. Lett.* **91**, 187902 (2003).
- [13] O. Oreshkov, T. A. Brun, and D. A. Lidar, *Phys. Rev. Lett.* **102**, 070502 (2009).
- [14] J. A. Jones, V. Vedral, A. Ekert, and G. Castagnoli, *Nature (London)* **403**, 869 (2000).
- [15] L. Faoro, J. Siewert, and R. Fazio, *Phys. Rev. Lett.* **90**, 028301 (2003).
- [16] Z. Y. Xue, J. Zhou, and Z. D. Wang, *Phys. Rev. A* **92**, 022320 (2015).
- [17] J. Zhang, T. H. Kyaw, D. M. Tong, E. Sjöqvist, and L. C. Kwek, *Sci. Rep.* **5**, 18414 (2015).
- [18] P. Zanardi and M. Rasetti, *Phys. Lett. A* **264**, 94 (1999).
- [19] J. T. Thomas, M. Lababidi, and M. Z. Tian, *Phys. Rev. A* **84**, 042335 (2011).
- [20] P. Solinas, P. Zanardi, N. Zanghi, and F. Rossi, *Phys. Rev. B* **67**, 121307(R) (2003).
- [21] L. A. Wu, P. Zanardi, and D. A. Lidar, *Phys. Rev. Lett.* **95**, 130501 (2005).
- [22] L. X. Cen, Z. D. Wang, and S. J. Wang, *Phys. Rev. A* **74**, 032321 (2006).
- [23] X. D. Zhang, Q. H. Zhang, and Z. D. Wang, *Phys. Rev. A* **74**, 034302 (2006).
- [24] S. L. Zhu and Z. D. Wang, *Phys. Rev. A* **67**, 022319 (2003).
- [25] Y. Xu, W. Cai, Y. Ma, X. Mu, L. Hu, T. Chen, H. Wang, Y. P. Song, Z. Y. Xue, Z. Q. Yin, and L. Sun, *Phys. Rev. Lett.* **121**, 110501 (2018).
- [26] M. V. Berry, *Proc. R. Soc. A* **392**, 45 (1984).
- [27] Y. Aharonov and J. Anandan, *Phys. Rev. Lett.* **58**, 1593 (1987).
- [28] F. Wilczek and A. Zee, *Phys. Rev. Lett.* **52**, 2111 (1984).
- [29] J. Anandan, *Phys. Lett. A* **133**, 171 (1988).
- [30] S. L. Zhu and P. Zanardi, *Phys. Rev. A* **72**, 020301(R) (2005).
- [31] S. Filipp, J. Klepp, Y. Hasegawa, C. Plonka-Spehr, U. Schmidt, P. Geltenbort, and H. Rauch, *Phys. Rev. Lett.* **102**, 030404 (2009).
- [32] Z. Zhu, T. Chen, X. Yang, J. Bian, Z. Y. Xue, and X. Peng, *Phys. Rev. Appl.* **12**, 024024 (2019).
- [33] P. Z. Zhao, G. F. Xu, Q. M. Ding, E. Sjöqvist, and D. M. Tong, *Phys. Rev. A* **95**, 062310 (2017).
- [34] Z. T. Liang, Y. X. Du, W. Huang, Z. Y. Xue, and H. Yan, *Phys. Rev. A* **89**, 062312 (2014).
- [35] G. F. Xu, P. Z. Zhao, D. M. Tong, and E. Sjöqvist, *Phys. Rev. A* **95**, 052349 (2017).
- [36] G. F. Xu, J. Zhang, D. M. Tong, E. Sjöqvist, and L. C. Kwek, *Phys. Rev. Lett.* **109**, 170501 (2012).
- [37] E. Sjöqvist, D. M. Tong, L. M. Andersson, B. Hessmo, M. Johansson, and K. Singh, *New J. Phys.* **14**, 103035 (2012).
- [38] G. Feng, G. Xu, and G. Long, *Phys. Rev. Lett.* **110**, 190501 (2013).
- [39] B. J. Liu, Z. H. Huang, Z. Y. Xue, and X. D. Zhang, *Phys. Rev. A* **95**, 062308 (2017).
- [40] Z. Y. Xue, J. Zhou, Y. M. Chu, and Y. Hu, *Phys. Rev. A* **94**, 022331 (2016).
- [41] Z. P. Hong, B. J. Liu, J. Q. Cai, X. D. Zhang, Y. Hu, Z. D. Wang, and Z. Y. Xue, *Phys. Rev. A* **97**, 022332 (2018).
- [42] X. K. Song, H. Zhang, Q. Ai, J. Qiu, and F. G. Deng, *New J. Phys.* **18**, 023001 (2016).
- [43] G. F. Xu, C. L. Liu, P. Z. Zhao, and D. M. Tong, *Phys. Rev. A* **92**, 052302 (2015).
- [44] G. F. Xu, P. Z. Zhao, T. H. Xing, E. Sjöqvist, and D. M. Tong, *Phys. Rev. A* **95**, 032311 (2017).
- [45] P. Z. Zhao, G. F. Xu, and D. M. Tong, *Phys. Rev. A* **94**, 062327 (2016).
- [46] P. Z. Zhao, G. F. Xu, and D. M. Tong, *Phys. Rev. A* **99**, 052309 (2019).
- [47] Y. H. Kang, Y. H. Chen, Z. C. Shi, B. H. Huang, J. Song, and Y. Xia, *Phys. Rev. A* **97**, 042336 (2018).
- [48] E. Herterich and E. Sjöqvist, *Phys. Rev. A* **94**, 052310 (2016).
- [49] V. A. Mousolou, C. M. Canali, and E. Sjöqvist, *New J. Phys.* **16**, 013029 (2014).
- [50] P. Z. Zhao, X. Wu, T. H. Xing, G. F. Xu, and D. M. Tong, *Phys. Rev. A* **98**, 032313 (2018).
- [51] B. J. Liu, X. K. Song, Z. Y. Xue, X. Wang, and M. H. Yung, *Phys. Rev. Lett.* **123**, 100501 (2019).
- [52] M. V. Berry, *J. Phys. A: Math. Gen.* **42**, 365303 (2009).
- [53] X. Chen, I. Lizuain, A. Ruschhaupt, D. Guéry-Odelin, and J. G. Muga, *Phys. Rev. Lett.* **105**, 123003 (2010).
- [54] A. del Campo, *Phys. Rev. Lett.* **111**, 100502 (2013).
- [55] K. Khodjasteh and D. A. Lidar, *Phys. Rev. Lett.* **95**, 180501 (2005).
- [56] A. M. Souza, G. A. Alvarez, and D. Suter, *Phys. Rev. Lett.* **106**, 240501 (2011).
- [57] G. T. Genov, D. Schraft, N. V. Vitanov, and T. Halfmann, *Phys. Rev. Lett.* **118**, 133202 (2017).
- [58] D. Daems, A. Ruschhaupt, D. Sugny, and S. Guérin, *Phys. Rev. Lett.* **111**, 050404 (2013).
- [59] X. T. Yu, Q. Zhang, Y. Ban, and X. Chen, *Phys. Rev. A* **97**, 062317 (2018).
- [60] E. S. Kyoseva and N. V. Vitanov, *Phys. Rev. A* **73**, 023420 (2006).
- [61] P. A. Ivanov and N. V. Vitanov, *Phys. Rev. A* **77**, 012335 (2008).
- [62] N. V. Vitanov, *Phys. Rev. A* **85**, 032331 (2012).
- [63] B. Rousseaux, S. Guerin, and N. V. Vitanov, *Phys. Rev. A* **87**, 032328 (2013).
- [64] X. Chen, E. Torrontegui, and J. G. Muga, *Phys. Rev. A* **83**, 062116 (2011).
- [65] X. Chen and J. G. Muga, *Phys. Rev. A* **86**, 033405 (2012).
- [66] U. Güngördü, Y. Wan, M. A. Fasihi, and M. Nakahara, *Phys. Rev. A* **86**, 062312 (2012).
- [67] E. Torrontegui, S. Martínez-Garaot, and J. G. Muga, *Phys. Rev. A* **89**, 043408 (2014).
- [68] S. Martínez-Garaot, E. Torrontegui, X. Chen, and J. G. Muga, *Phys. Rev. A* **89**, 053408 (2014).

- [69] Y. H. Kang, Y. H. Chen, Z. C. Shi, B. H. Huang, J. Song, and Y. Xia, *Phys. Rev. A* **97**, 033407 (2018).
- [70] Y. H. Kang, Z. C. Shi, B. H. Huang, J. Song, and Y. Xia, *Phys. Rev. A* **100**, 012332 (2019).
- [71] Y. H. Kang, B. H. Huang, P. M. Lu, and Y. Xia, *Laser Phys. Lett.* **14**, 025201 (2017).
- [72] Y. C. Li, D. Martínez-Cercós, S. Martínez-Garaot, X. Chen, and J. G. Muga, *Phys. Rev. A* **97**, 013830 (2018).
- [73] Y. C. Li, X. Chen, J. G. Muga, and E. Y. Sherman, *New J. Phys.* **20**, 113029 (2018).
- [74] A. del Campo, M. M. Rams, and W. H. Zurek, *Phys. Rev. Lett.* **109**, 115703 (2012).
- [75] Y. H. Chen, Y. Xia, Q. Q. Chen, and J. Song, *Phys. Rev. A* **89**, 033856 (2014).
- [76] Y. H. Chen, Y. Xia, Q. Q. Chen, and J. Song, *Phys. Rev. A* **91**, 012325 (2015).
- [77] Y. X. Du, Z. T. Liang, H. Yan, and S. L. Zhu, *Adv. Quantum Technol.* **2**, 1900013 (2019).
- [78] D. M. Zajac, A. J. Sigillito, M. Russ, F. Borjans, J. M. Taylor, G. Burkard, and J. R. Petta, *Science* **359**, 439 (2018).
- [79] F. A. Calderon-Vargas, G. S. Barron, X. H. Deng, A. J. Sigillito, E. Barnes, and S. E. Economou, *Phys. Rev. B* **100**, 035304 (2019).
- [80] H. R. Lewis and W. B. Riesenfeld, *J. Math. Phys.* **10**, 1458 (1969).
- [81] R. S. Kaushal and H. J. Korsch, *J. Math. Phys.* **22**, 1904 (1981).
- [82] S. Ahmad and A. Ambrosetti, First order linear differential equations, *A Textbook on Ordinary Differential Equations*, Vol. 88 (Springer, Cham, 2015).
- [83] F. Martins, F. K. Malinowski, P. D. Nissen, E. Barnes, S. Fallahi, G. C. Gardner, M. J. Manfra, C. M. Marcus, and F. Kuemmeth, *Phys. Rev. Lett.* **116**, 116801 (2016).
- [84] M. D. Reed, B. M. Maune, R. W. Andrews, M. G. Borselli, K. Eng, M. P. Jura, A. A. Kiselev, T. D. Ladd, S. T. Merkel, I. Milosavljevic, E. J. Pritchett, M. T. Rakher, R. S. Ross, A. E. Schmitz, A. Smith, J. A. Wright, M. F. Gyure, and A. T. Hunter, *Phys. Rev. Lett.* **116**, 110402 (2016).
- [85] T. Chen, J. Zhang, and Z. Y. Xue, *Phys. Rev. A* **98**, 052314 (2018).
- [86] A. Miranowicz, S. K. Özdemir, J. Bajer, G. Yusa, N. Imoto, Y. Hirayama, and F. Nori, *Phys. Rev. B* **92**, 075312 (2015).